1    *Article*

2  # Kū Hou Kuapā: Cultural restoration improves water
3  # budget and water quality dynamics in Heʻeia
4  # Fishpond

5    **Paula Mohlenkamp [1], Charles Kaiaka Beebe [1], Margaret A. McManus [1], Angela Hiʻilei Kawelo [2],**
6    **Keliʻiahonui Kotubetey [2], Mirielle Lopez-Guzman [1,3], Craig E. Nelson [1,3,4], Rosanna ʻAnolani**
7    **Alegado [1,3,4,*]**

8    [1]  Department of Oceanography, University of Hawaiʻi Mānoa, Honolulu, HI 96822, USA;
9         pmoehlen@hawaii.edu (P.M.); cbeebe@hawaii.edu (C.K.B.); mamc@hawaii.edu (M.A.M); malg@hawaii.edu
10        (M.L.-G.); craig.nelson@hawaii.edu (C.E.N.)
11   [2]  Paepae o Heʻeia, Kāneʻohe, HI 96744, USA; hiilei@paepaeoheeia.org (A.H.K.); kelii@paepaeoheeia.org
12        (K.K.)
13   [3]  Daniel K. Inouye Center for Microbial Oceanography: Research and Education, University of Hawaiʻi
14        Mānoa, Honolulu, HI 96822, USA;
15   [4]  Sea Grant College Program, University of Hawaiʻi, Mānoa, Honolulu, HI 96822
16   *  Correspondence: rosie.alegado@hawaii.edu; Tel.: +01-808-956-0565

17

18

19   **Abstract:** In Hawaiʻi, the transition from customary subsistence flooded taro agroecosystems,
20   which regulate stream discharge rate trapping sediment and nutrients, to a plantation-style
21   economy (c. the 1840s) led to nearshore sediment deposition - smothering coral reefs and destroying
22   adjacent coastal fisheries and customary fishpond mariculture. To mitigate sediment transport,
23   *Rhizophora mangle* was introduced in estuaries across Hawaiʻi (c. 1902) further altering fishpond
24   ecosystems. Here, we examine the impact of cultural restoration between 2012-2018 at Heʻeia
25   Fishpond, a 600-800-year-old walled fishpond. Fishpond water quality was assessed by calculating
26   water exchange rates, residence times, salinity distribution, and abundance of microbial indicators
27   prior to and after restoration. We hypothesized that *R. mangle* removal and concomitant
28   reconstruction of sluice gates would increase mixing and decrease bacterial indicator abundance in
29   the fishpond. We find that Heʻeia Fishpond's physical environment is primarily tidally driven;
30   wind forcing and river flux are secondary drivers. Post-restoration, two gates in the northeastern
31   region account for >80% of relative flux in the fishpond. Increase in exchange rates during spring
32   and neap tide and shorter minimum water residence time corresponded with the reconstruction of
33   a partially obstructed 56 m gap together with the installation of an additional sluice gate in the
34   fishpond wall. Lower mean salinities post-restoration suggests increased freshwater influx due to
35   *R. mangle* removal. Spatial distribution of microbial bio-indicator species inversely correlated with
36   salinity. Average abundance of *Enterococcus* and *Bacteroidales* did not significantly change after
37   restoration efforts, however, average abundance of a biomarker specific to birds nesting in the
38   mangroves decreased significantly after restoration. This study demonstrates the positive impact of
39   biocultural restoration regimes on water flushing and water quality parameters, encouraging the
40   prospect of revitalizing this and other culturally and economically significant sites for sustainable
41   aquaculture in the future.

42   **Keywords:** mariculture; aquaculture; community restoration; conservation ecology; Native
43   Hawaiian fishpond; microbes; microbial source tracking

44

45

46   **1.0 Introduction**

47   *1.1 Native Hawaiian fishpond mariculture and food security*

48   As the catch rate of our global fisheries levels off due to degradation of the environment and
49   even collapse of specific fish populations, the demand for aquaculture production of fish is projected
50   to increase markedly [1]. Concerns over sustainable food production have brought indigenous
51   models of resource management to the fore. Hawai'i currently imports about half of our seafood [2]
52   and local aquaculture is estimated to supply only ~20,000 lbs annually [3], but this was not always
53   the case. For centuries, Native Hawaiians developed marine aquaculture that utilized natural
54   enrichments via freshwater from surface and submarine groundwater discharge in managed
55   estuaries, fishponds (*loko i'a*) [4]. These walled fishponds (*loko i'a kuapā*) were intentionally built in
56   natural embayments at the interface of freshwater streams and the ocean where nutrients from
57   streams promoted the growth of primary producers in constrained brackish ecosystems. The kuapā
58   regulates freshwater inflow to size slotted sluice gates (*mākāhā*), creates a low wave energy
59   environment within the fishpond, impedes water flux into and out of the fishpond and ensures that
60   a minimum volume of water is retained in the fishpond at all times, especially at extremely low tides.
61   In this system, unicellular photosynthetic microbes form the base of a complex food web that yielded
62   energetically efficient protein production of crustaceans and herbivorous fish species. Fishpond
63   stewards (*kia'i loko i'a*) practiced stock enhancement, leveraging knowledge of juvenile fish
64   migration to trap target species behind mākāhā until reaching maturity and preventing entry of large
65   predators. In addition, kia'i loko regulate flux or harvest fish by blocking mākāhā. It is estimated
66   that fishponds in Hawai'i could have yielded approximately 2 million pounds of fish per year total
67   historically [5,6].

68   *1.2 The legacy of land use change and invasive species on loko i'a*

69   Physical changes (sedimentation, storm damage, development, disuse) and biological invasions
70   have dramatically altered many loko i'a. Beginning in the 1800s, a shift from subsistence to plantation
71   economy led to erosion and siltation of the nearshore environment. In an attempt to mitigate and
72   stabilize these impacts, mangroves were introduced to Hawai'i in 1902 [7]. Mangroves are highly
73   appreciated in their native habitats for the ecosystem services they provide throughout the tropics -
74   shoreline protection and sediment stabilization [8], litterfall subsidy [9] and provision of nursery
75   grounds [8]. Thus, by modifying their environment, mangroves have cascading effects for resident
76   biota, acting as important ecosystem engineers.
77   However, in Hawai'i, mangroves have caused a variety of negative ecological and economic
78   impacts that motivate their removal [10]. Mangrove's preference for halotypic ecotones favor their
79   growth in estuaries with their root systems obstructing mākāhā, decreasing water velocity, flushing,
80   circulation and residence time of loko i'a and the streams that feed them [11–13]. Instead of sandy
81   habitats, mangrove vegetated areas have high sedimentation rates and anoxic sediments due to
82   bacterial decomposition of mangrove leaf detritus [11,14]. Moreover, mangrove draws down
83   nitrogen and phosphate and decrease dissolved oxygen from overlying waters, potentially inhibiting
84   primary production rates in loko i'a   [13]. Importantly, the absence of mangrove feeding specialists
85   in Hawai'i have resulted in poor assimilation of mangrove-derived nutrients from introduced stands
86   [15] because detritivores native to Hawai'i are not adapted to utilizing mangrove detritus, which
87   tends to be tannin-rich and nitrogen-poor [16].
88   Post-World War II, a combination of urbanization, the introduction of invasive species, as well
89   as stochastic events (e.g., storms, floods, tsunamis and lava flows) resulted in widespread
90   deterioration of Hawaiian fishponds across the state [6]. By 1977, only 28 loko i'a were still in
91   production and by 1985, merely 7 loko i'a were in commercial or subsistence use [6]. The loss of
92   actively maintained loko i'a exacerbated the spread of invasive mangrove in coastal estuaries [17].

93   *1.3 Biocultural restoration of loko i'a: He'eia Fishpond as a model*

94   Driven by a desire to re-establish customary practices, provide economic opportunities to local
95   communities and improve production of crustaceans and herbivorous fish, a grassroots movement

96   of loko iʻa restoration has gained momentum since the early 2000s [18–20]. Hui Malama Loko Iʻa is
97   a statewide network of indigenous kiaʻi loko dedicated to restoring loko iʻa for food production [21].
98   Loko iʻa restoration generally entails mangrove removal and dry stacking of basalt with coral/rubble
99   internally. Typical mangrove clearing practices in Hawaiʻi include the removal of the above-
100  sediment mangrove biomass, leaving intact the prop roots and the root-fiber mat within the sediment.
101  Despite the increase in loko iʻa restoration across the state, we know of no published data on the
102  effects of mangrove removal and loko iʻa infrastructure repair on water circulation dynamics and
103  water quality.
104      Located on the windward side of Oʻahu Island, Hawaiʻi (Figure 1A), Heʻeia Fishpond (also
105  known as Pihi Loko Iʻa) is a loko iʻa kuapā estimated to have been built 600-800 years ago atop the
106  Malaukaʻa fringing reef [22] and has been at the forefront of fishpond restoration in Hawaiʻi.
107  *Rhizophora mangle* was introduced to the Heʻeia estuary in 1922 to control runoff from upstream
108  agriculture and stabilize sediments [11,15]. The circulation and flux patterns within Heʻeia Fishpond
109  were compromised during the Keapuka Flood. On May 2, 1965, the highest discharge rate on record
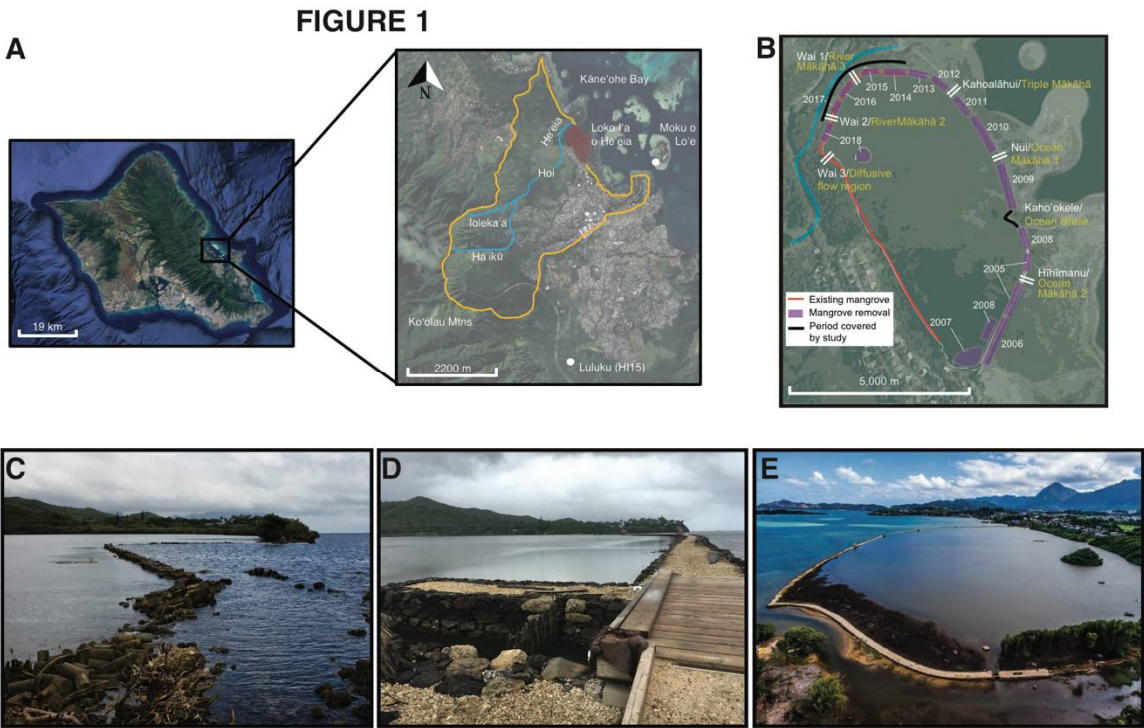


110  from Haʻikū and ʻIolekaʻa streams occurred during the Keapuka Flood [23]. Flood waters first broke
111  the kuapā in the northwestern sector adjacent to Heʻeia Stream, creating a 183 m opening in the loko
112  iʻa wall. Historical tidal data [24] indicate that the flood likely occurred during a perigean spring tide
113  (a. k. a. King Tide), thus the build-up of internal pressure within the loko iʻa coupled with an
114  extremely low tide outside the loko iʻa, likely caused a 56 m break in the kuapā on eastern seaward
115  side as well (Figure 1B, "Ocean Break").

116      **Figure 1. Study site: Heʻeia ahupuaʻa and fishpond. ()** The Heʻeia *ahupuaʻa* (social-
117      political governance unit, usually organized along watershed boundaries) is located on the
118      northeast/windward side of Oʻahu Island, HI. Heʻeia ahupuaʻa is outlined in yellow,
119      Heʻeia Stream (blue line) originates as Haʻikū Stream near the ridgeline of the Koʻolau
120      Mountains and converges with Iolekaʻa Stream before entering Hoi wetlands and flowing
121      into and past Heʻeia Fishpond (shaded red) into Kāneʻohe Bay. Weather stations on Moku
122      o Loʻe and Luluku (HI15) rain gauge are indicated by white dots. (map downloaded from
123      USGS National Map Viewer) **(B) Bio-cultural restoration over the course of this study.**
124      Freshwater and marine inputs into Heʻeia fishpond via mākāhā (sluice gate) locations and
125      names, yellow: community stewards Paepae o Heʻeia, white: Heʻeia Coastal Ocean
126      Observing System; time period of this study (black line) in the context of the

127　　　chronosequence of mangrove removal and wall rebuilding. From 1965 - 2015 a 100 m break
128　　　in the kuapā (**C**) altered flow patterns in the fishpond. From 2014-2015, Paepae o Heʻeia
129　　　(POH) and community volunteers repaired the kuapā and built a mākāhā (Kahoʻokele)
130　　　(**D**). (**E**) From 2014-2017, POH removed invasive *R. mangle* and repaired kuapā and mākāhā
131　　　infrastructure on the north quadrant of the fishpond bordering Heʻeia Stream (photo
132　　　courtesy of Sam Kapoi).

133　　　　As a result of the shift from a constrained to a radically unconstrained system, the fundamental
134　　functioning of the loko iʻa changed:　the volume became strongly tidally dominated and fish
135　　production using customary mariculture techniques could no longer be practiced. A dense mangrove
136　　forest around the mouth of Heʻeia stream expanded into the loko iʻa, growing along and eventually
137　　obscuring the kuapā and effectively decreasing the amount of surface freshwater delivered to the
138　　loko iʻa. Sediment loading from Heʻeia Stream, agriculture and urbanization overwhelmed the
139　　original mechanisms by which material was flushed out of the loko iʻa [25]. Progressive
140　　accumulation of terrigenous particulates on the coral benthos, accelerated by a dense mangrove root
141　　mass decreased the average fishpond depth to ~1 m [26]. These conditions - increased salinity, organic
142　　matter, and turbidity likely facilitated a shift in the biological diversity and composition of the loko
143　　iʻa away from desirable aquaculture species and toward invasive macroalgae.
144　　　　Though limited restoration in the past 25 years enabled conventional net pen aquaculture in the
145　　loko iʻa, the ecosystem became steadily more eutrophic. In 1988, Mark Brooks leased the fishpond,
146　　installing a 0.9 m retaining wall of cement cinder blocks that reduced the tidal influence and
147　　prevented water exchange except at spring tides (Figure 1C). In addition, a previous flood in 1927
148　　deposited a portion of the kuapā into the interior of the loko iʻa creating a mangrove stand where a
149　　2,000-3,000 introduced cattle egrets *(Bubulcus ibis)* established a rookery (Fig 1B). The potential for
150　　human and animal health impacts from microbial contamination is a central concern in maintaining
151　　an ecologically balanced and productive loko iʻa [27,28]. Limited circulation within Heʻeia
152　　exacerbates this issue, particularly from given the rich source of guano and nutrients produced by
153　　the egret colony.
154　　　　In the present study, we partnered with the non-profit organization Paepae o Heʻeia, kiaʻi loko
155　　of Heʻeia Fishpond, to assess the impacts of restoration from 2012-2018. Since 2001, Paepae o Heʻeia
156　　has sought to foster cultural sustainability and restore and maintain a thriving fishpond for the local
157　　community by linking traditional knowledge and contemporary management practices. With the
158　　help of over 50,000 community volunteers, Paepae o Heʻeia has resurrected the kuapā along its
159　　historical footprint and progressively removed over 2 km of invasive *R. mangle* (Figure 1B-1E). In this
160　　contribution, we addressed the following questions: 1) How does kuapā infrastructure repair
161　　including mangrove clearance around the fishpond periphery affect circulation dynamics such as
162　　water exchange rates, residence time? 2) How does the potential for increased freshwater and marine
163　　inputs alter the overall salinity distribution of the loko iʻa? and 3) How do these changes in the
164　　physical characteristics of water in the loko iʻa alter microbial bioindicators for fecal contamination?

## 2. Methods and Materials

### 2.1 Study site

167　　　　Heʻeia Fishpond (21°26′10.74″ N, 157°48′28.05″W) is a 0.356 km$^2$ embayment located on the
168　　windward side of Oʻahu Island, Hawaiʻi (Fig 1A). The loko iʻa is completely enclosed by 2.5 km of
169　　kuapā and is bordered by Kāneʻohe Bay to the south and east, Heʻeia Stream to the north, and a
170　　remnant irrigation ditch (*auwai*) running longitudinally along its entire west bank. The Haʻikū
171　　Stream near the ridgeline of the Koʻolau Mountains converges with the ʻIolekaʻa Stream and
172　　becomes Heʻeia Stream before entering the Hoi wetland. Within the Hoi wetlands, a portion of
173　　Heʻeia Stream is diverted through a network of *auwai*, irrigating taro patches. At the terminus of the
174　　watershed, Heʻeia Stream historically splits, either flowing south in the auwai that parallels Heʻeia
175　　Fishpond or east toward Kāneʻohe Bay. A forest of *R. mangle* occupies the northwest and western
176　　periphery of Heʻeia Fishpond.

177    Mākāhā are interspersed along the kuapā, connecting the fishpond to exterior water sources and
178    regulating surface and seawater exchange with the fishpond (Figure 1B, Table 1). Hereafter, names
179    of mākāhā follow the convention used by Paepae o Heʻeia. Designations from previous studies
180    [29,30] are also given. For the past 50 years, mākāhā channels in Heʻeia Fishpond have concrete floors
181    with vertical walls composed of basalt and coral rubble with either a semi-permeable barrier fence or
182    grid constructed from wood or plastic (Figure 2). With the exception of Kahoʻokele, the floor of the
183    mākāhā are slightly higher than the natural bottom of the loko iʻa. All fieldwork was conducted with
184    the permission of Paepae o Heʻeia and the private landowner, Kamehameha Schools (Joey Char,
185    Land Asset Manager, Kamehameha Schools Community Engagement and Resources Division).

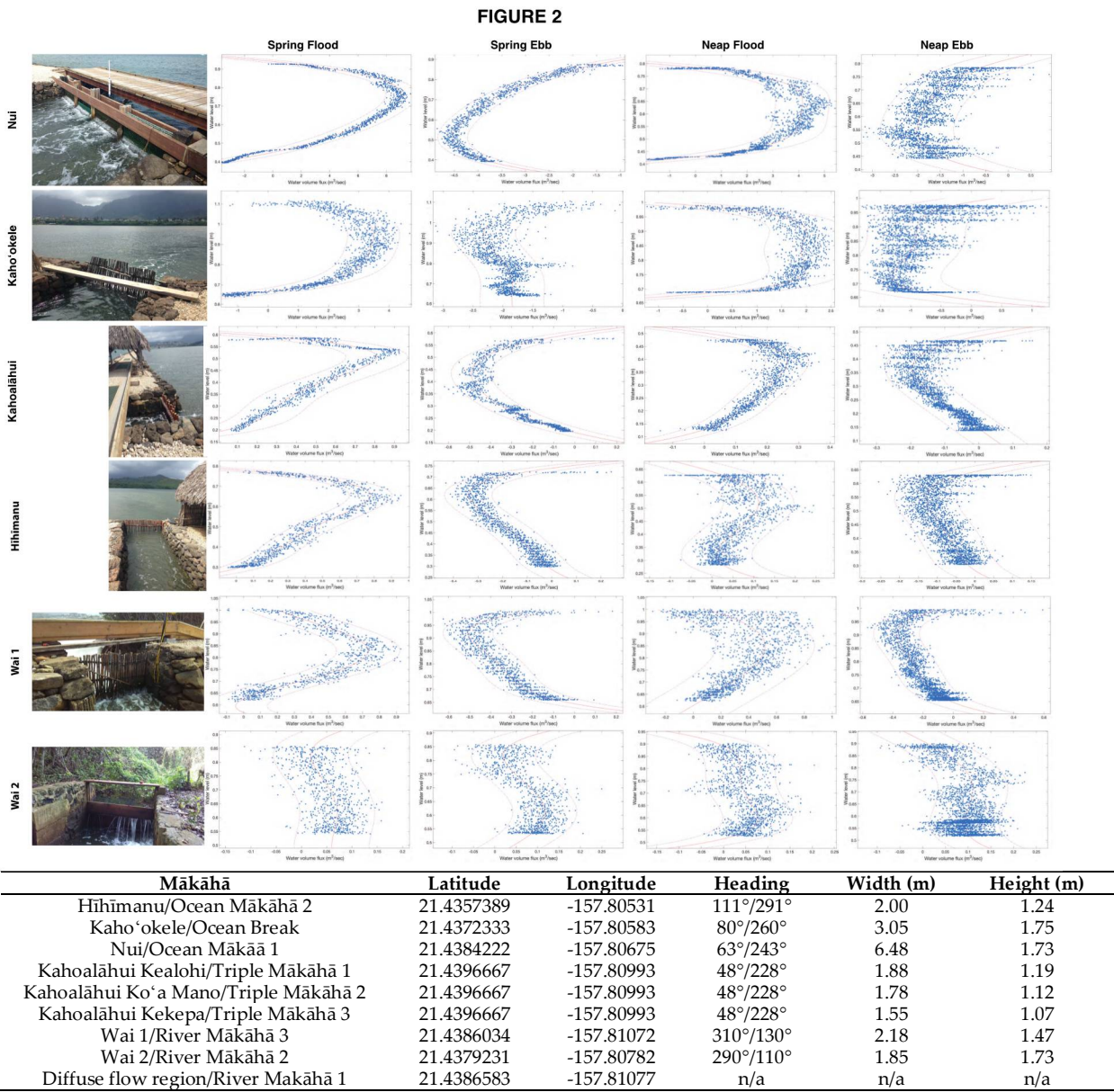186    **Table 1.** Mākāhā locations, heading, and dimensions.



**FIGURE 2**

| Mākāhā | Latitude | Longitude | Heading | Width (m) | Height (m) |
|---|---|---|---|---|---|
| Hīhīmanu/Ocean Mākāhā 2 | 21.4357389 | -157.80531 | 111°/291° | 2.00 | 1.24 |
| Kahoʻokele/Ocean Break | 21.4372333 | -157.80583 | 80°/260° | 3.05 | 1.75 |
| Nui/Ocean Mākāā 1 | 21.4384222 | -157.80675 | 63°/243° | 6.48 | 1.73 |
| Kahoalāhui Kealohi/Triple Mākāhā 1 | 21.4396667 | -157.80993 | 48°/228° | 1.88 | 1.19 |
| Kahoalāhui Koʻa Mano/Triple Mākāhā 2 | 21.4396667 | -157.80993 | 48°/228° | 1.78 | 1.12 |
| Kahoalāhui Kekepa/Triple Mākāhā 3 | 21.4396667 | -157.80993 | 48°/228° | 1.55 | 1.07 |
| Wai 1/River Mākāhā 3 | 21.4386034 | -157.81072 | 310°/130° | 2.18 | 1.47 |
| Wai 2/River Mākāhā 2 | 21.4379231 | -157.80782 | 290°/110° | 1.85 | 1.73 |
| Diffuse flow region/River Makāhā 1 | 21.4386583 | -157.81077 | n/a | n/a | n/a |

187    **Figure 2. Post-restoration rating curves at each mākāhā over various tidal stages.** Water
188    volume flux (m³ s⁻¹) relative to the water level (m) is shown for all 6 mākāha, ʻbest fit lineʻ
189    in red, 9% confidence intervals, dashed pink line. Positive values indicate flux and negative
190    values indicate flux out of the fishpond.

191

192      *2.2 Mass-flux and volume change calculations*

193          To evaluate the current direction (°), water level (m) and water velocity (m s⁻¹) into and out of
194      the fishpond, Sontek Argonaut Shallow Water (SW) Profilers (SonTek, San Diego, CA) were deployed
195      over the course of 7 days in each mākāhā (Fig 2, Table S1). The Argonaut SW Profiler and battery
196      housing was oriented facing into the channel and mounted to 0.7 x 0.7 m metal mooring with ~25 kg
197      weights and placed at the bottom of each mākāhā channel. Several flood and ebb tide tidal cycles
198      were recorded to capture one full neap and spring tide using a high-frequency measurement interval
199      of 20 s with an averaging interval of 10 s. The blanking distance was set to the minimal amount of
200      0.07 m, as the mean water column was < 0.50 m.
201          Precipitation, tidal state, wind direction, and speed were used as criteria for selecting pre- and
202      post-restoration dates (Table S2). Daily (cm 24 hrs⁻¹) and cumulative precipitation over 4 days (cm 96
203      hrs⁻¹) obtained from the National Oceanic and Atmospheric Administration Luluku (HI15) rain
204      gauge station (http://www.prh.noaa.gov/hnl/hydro/hydronet/hydronet-data.php) consistent with
205      previous studies [30,31]. Mean stream streamflow (mean m³ s⁻¹ 24 hrs⁻¹) calculated using data from
206      US Geological Survey discharge station (Haʻikū Station #16275000) accessed from
207      http://waterdata.usgs.gov. Wind direction and magnitude was determined from automatic weather
208      station *Moku o Loʻe* (21.4339° N, 157.7881° W), 1.5 km from Heʻeia Fishpond
209      (http://www.pacioos.hawaii.edu/weather/obs-mokuoloe/). The station is positioned ~5 m above sea
210      level and is outfitted with an Eppley 295-385 nm ultraviolet (UV) radiometer, a LiCor 200SZ
211      Pyranometer, and a LiCor Quantameter (400-700 nm). A sea level gauge with a water temperature
212      probe, located ~ 10 m offshore of the weather station at a depth of ~ 1 m, was used for tidal data
213      (http://tides.mobilegeographics.com/locations/3854.html).
214          Flux data and water velocity measurements (m s⁻¹) acquired from the Sontek Argonaut SW
215      Profiler were used to generate rating curves for each mākāhā at each tidal state (spring flood tide, SF;
216      spring ebb tide, SE; neap flood tide, NF; and neap ebb tide, NE) using the following equation:

$$\phi = wdv, \tag{1}$$

217      where w is the respective mākāhā width (m), d is the water level vector (m) changing over time with
218      the tide, and v is the water velocity (m s⁻¹) through the mākāhā channel [29,30]. To account for
219      bidirectional water flow in the mākāhā due to tidal forcing, water volume flux was determined for
220      an entire tidal cycle at the following tidal stages: SF, SE, NF, and NE. Full tidal amplitude was used
221      when splitting the data set based on tidal stage. Rating curves were fitted using a poly-fit function
222      with a best-fit line and 95% confidence intervals in Matlab (The MathWorks Inc., Natick, MA). Here,
223      flux values for Kahoalāhui/Triple Mākāhā were calculated by taking flow measurements at the
224      northernmost mākāhā channel (Kealohi) and multiplying by three.
225          Based on water volume flux, mean and maximum flow through each mākāhā were calculated
226      for four tidal cycles (SF, SE, NF, NE). To account for varying tidal cycle length caused by mixed
227      semidiurnal tides in Kāneʻohe Bay, individual mākāhā flow rates were normalized by calculating
228      the total volume of water (m) moving through a mākāhā channel at a given tidal cycle and the hourly
229      flux rate.
230          Fishpond volume was calculated using 728 bathymetric depth measurements normalized to
231      mean low low water from a reference HOBO® water level logger (Onset, Bourne, MA) deployed at
232      an interior site within the fishpond (21.43466° N, W 157.80699° W) that recorded tidal fluctuations
233      during bathymetry mapping [26], Timmerman *et al.*, unpublished. In 2018, we deployed a HOBO®
234      water level logger at the same location to recollect reference water level data over a 10-day period.
235      Reference pressure data was corrected for atmospheric pressure fluctuations using a second HOBO
236      logger situated on land to record atmospheric pressure fluctuations.
237          To calculate post-restoration loko iʻa volume, the difference in reference tidal state from pre-
238      restoration (2007) and post-restoration (2018) was applied to the bathymetry dataset at SF, SE, NF,
239      NE tidal states with Station *Moku o Loʻe* as a reference. A rectangular grid with ~1 m spacing and a
240      natural neighbor interpolation was adopted to estimate depths in between measured bathymetry
241      points in Matlab. For each tidal state, a trapezoidal rule was used with no smoothing applied. The
242      small mangrove island located in the northwest quadrant of the fishpond was excluded from our
243      calculations.

244  To derive minimum residence time in Heʻeia Fishpond, the amount of water exchanged during
245  ebb flood transition was calculated for neap and spring tide using the following equations [30]:

$$\tau_{HFS} = \frac{\text{He}\,'\,\text{eia Fishpond Volume Exchanged (spring high tide – spring low tide)}}{\text{He}\,'\text{eia Fishpond Volume (spring high tide)}}, \qquad (2)$$

$$\tau_{HFN} = \frac{\text{He}\,'\,\text{eia Fishpond Volume Exchanged (neap high tide – neap low tide)}}{\text{He}\,'\text{eia Fishpond Volume (neap high tide)}}, \qquad (3)$$

246  To determine residence time, the following assumptions were made: fishpond water column is mixed
247  uniformly, all flood and ebb tides are 6 hours long, and mākāhā are the only source of water exchange
248  with the following equation,

$$\varphi^x = 0.01, \qquad\qquad (4)$$

249  where $\varphi$ is the percentage of water remaining after 1 flushing cycle (12 hours) and x is the residence
250  time in flushing cycles.

251  *2.3 Sampling regime*

252  This study utilized on-going efforts by Nā Kilo Honua o Heʻeia (http://nakilohonua.org), a
253  Heʻeia coastal ocean observing research collective at the University of Hawaiʻi at Mānoa, which has
254  carried out monthly sampling at Heʻeia Fishpond since 2007 [29] to collect discrete samples. To
255  minimize the variability of physical and chemical characteristics of the loko iʻa due to tidal exchange,
256  samples were collected during neap tide over a period of 3-4 hr. The pre-restoration (2014) sampling
257  grid was comprised of 10 stations within the fishpond (P1–P10) whereas the post-restoration (2017)
258  sampling grid was comprised of 11 stations within the fishpond (L01-L10), each of the intact mākāhā
259  (M01–M06), Tables S3 and S4 respectively. Reference endmembers for oceanic input were taken
260  outside the kuapā at Kahoʻokele/Ocean Break (E01) whereas endmembers for surface freshwater
261  were collected in Heʻeia Stream between the Hoi wetland and Heʻeia Fishpond outside the kuapā
262  (E02). To minimize the disturbance of the water column and benthos prior to measurements, stations
263  were approached against prevailing currents and winds. Salinity was measured using a YSI
264  Professional Plus (ProPlus) multiparameter sonde (YSI Xylem Brand, Yellow Springs, OH). At each
265  station, a measurement was taken ~ 5-10 cm below the water surface ("surface") and 5-10 cm above
266  the benthos ("bottom") by allowing the instrument reading to stabilize for 2-3 minutes before
267  recording values.
268  Eleven stations were selected for discrete sampling for microbes: Kahoʻokele/Ocean Break, Wai
269  1, and 9 stations in the fishpond interior. Pre-restoration (P01-P10, Ocean Break) and post-restoration
270  (L01-L03, L06-L11, Kahoʻokele, Wai 2) locations differed slightly (Table S3, Figure 5A). At each
271  station, 1L polycarbonate bottles were acid washed and rinsed with ambient surface water three
272  times, before immersion at the surface to fill the bottle completely. Samples were stored at 4 °C and
273  processed within 2 hr of collection. Seawater was filtered through a 47 mm diameter, 0.45 μm filter
274  (MCE, Millipore, Sigma, Burlington, MA) and stored at -80 °C prior to DNA extraction.

275  *2.4 Microbial source tracking*

276  Total genomic DNA (gDNA) was extracted from filters using the PowerWater DNA Extraction
277  kit (QIAGEN, Germantown, MD) following the manufacturer's instructions. Quantitative PCR
278  (qPCR) was used to determine the abundance of bacterial 16S rRNA genes from mammalian fecal
279  indicator bacteria *Enterococcus* using assay Entero1a [32–34] and Bacteroidales using assay GenBac3
280  *[35–37]*. Quantification was performed with the KAPA PROBE FORCE qPCR system (Wilmington,
281  MA) using KAPA PROBE FORCE qPCR Master Mix (20 μL reactions), 400 nM specific Taqman
282  primers (Table 2) and template gDNA diluted 1:5. Standards were run in triplicate using an 8-point,
283  5-fold serial dilution. Cycling parameters for all assays were: 95 °C for 2 min, 45 cycles of 95 °C for 15
284  sec and annealing/extension at 60 °C for 30 sec. Ct values were converted to concentrations per 100
285  mL using the manufacturer's software. The standards used for the Entero1a and GenBac3assays were

286 genomic DNA extracted from *Enterococcus faecalis* strain V583 (ATCC® 700802D-5™) and *Bacteroides*
287 *thetaiotaomicron* strain VPI 5482 (ATCC® 29148™), respectively.
288     Primers previously shown to detect avian fecal contamination in water [38] were tested on *B.*
289 *ibis* fecal DNA (Table 2). Briefly, fecal material was collected from birds present on the small
290 mangrove island on the loko iʻa interior. Total genomic DNA was extracted from avian feces using
291 the DNeasy PowerSoil Kit (QIAGEN, Germantown, MD) following the manufacturer's instructions.
292 qPCR using GFC primers targeting the 16S rRNA gene from *Catellicoccus marimammalium* used the
293 KAPA SYBR FAST qPCR system (20 µL reactions), 400 nM primers, and gDNA diluted 1:5. Cycling
294 parameters were as follows: 95 °C for 3 min for enzyme activation, followed by 40 cycles of 95 °C for
295 3 sec and annealing/extension at 60 °C for 20 sec. Ct values were calculated as previously described
296 with uncultured *Catellicoccus* sp. 16S rRNA gene, partial sequence (Genbank accession number
297 JN084062) used as a standard.

298     **Table 2.** 16S rDNA oligos used in this study.

| Target | Primer | Sequence | Ref. |
|--------|--------|----------|------|
| *Enteroccocus* | Entero1af | AGAAATTCCAAACGAACTTG | [32, 33, 34] |
| | Entero1ar | CAGTGCTCTACCTCCATCATT | [32, 33, 34] |
| | Entero1ap | 6-FAM™/TGGTTCTCT/ZEN™/CCGAAATAGCTTTAGGGCTA/IB®FQ/ | [32, 33, 34] |
| Bacteroidales | GenBac3f | GGGGTTCTGAGAGGAAGGT | [35, 36, 37] |
| | GenBac3r | CCGTCATCCTTCACGCTACT | [35, 36, 37] |
| | GenBac3p | 6-FAM™/CAATATTCC/ZEN™/TCACTGCTGCCTCCCGTA/IB®FQ/ | [35, 36, 37] |
| *Catellicoccus* | GFCf | CCC TTG TCG TTA GTT GCC ATC ATT C | [38] |
| *marimammalium* | GFCr | GCC CTC GCG AGT TCG CTG C | [38] |

299 *2.5 Statistics*

300     Statistical significance for pre- and post-restoration events was determined with a pairwise
301 Welchʻs t-test to account for differences in variance. Mean baseline events pre-restoration and mean
302 baseline events post-restoration for salinity and log-transformed numbers of microbial biomarker
303 abundance were compared with the t-test for statistical significance in R (R Foundation for Statistical
304 Computing) with the p-value for statistical significance set to $p < 0.05$. In addition, correlation of
305 GFC/GenBac3/Entero1a distribution with salinity, date, and location was tested using a generalized
306 additive mixed model (GAMM) in R (R Foundation for Statistical Computing). Mean baseline salinity
307 and log-transformed numbers of microbial biomarker abundance pre- and post-restoration was
308 plotted with a contour plot function in Matlab (The MathWorks Inc., Natick, MA).

309 **3. Results**

310 *3.1 Restoration from 2014-2018 shifted relative flux contributions of each mākāhā*

311     Before the restoration, fish movement could not be regulated using the mākāhā system. Thus,
312 Paepae o Heʻeia centered their research, education, and aquaculture activities around quarter-acre
313 net pens. From 2006-2009 Paepae o Heʻeia produced approximately 1.2 metric tons of Pacific
314 threadfin. Two events occurred in 2009, in which there was massive fish mortality. These events
315 prompted a re-evaluation of the use of conventional rearing techniques in Heʻeia Fishpond.
316 Repairing the kuapā would eliminate the need for net pen aquaculture, enabling fish stock to move
317 throughout the entire fishpond toward cooler and/or more oxygenated areas in response to future
318 environmental stress. Moreover, Paepae o Heʻeia hypothesized that consistent freshwater input and
319 nutrients, via functional mākāhā would increase primary productivity and subsequently increase the
320 biomass of native herbivores in the loko iʻa. Biocultural restoration from 2012 to 2018 targeted the
321 gap in the seaward kuapā and the section bordering Heʻeia Stream (Figure 1B).
322     The restoration phase involving repair of the 56 m kuapā gap spanned 2014-2015 and was known
323 as *Pani ka puka* (Shut the door). Kiaʻi loko used traditional external materials (*pohaku pele*, basalt rock)
324 and a mix of traditional and contemporary internal materials (*koʻa*, coral rubble, and remnant cinder
325 blocks) to rebuild the north and south segments of broken kuapā simultaneously and meeting in the
326 middle. Rather than rebuild a continuous kuapā spanning the entire seaward wall of the loko iʻa,
327 Paepae o Heʻeia elected to install a new mākāhā (Kahoʻokele) to increase fishpond circulation,

328   increase oxygenation of the water column, and promote recruitment of marine species (Fig 1 C-D).
329   Mākāhā site selection was based on empirical kia'i loko observations of areas with the highest
330   abundance and diversity of marine life (ex. fish, oysters, macroalgae, sponges). Per Bernoulli's
331   principle, as the kuapā gap narrowed, the velocity of water exchange increased, scouring the bottom
332   of the new mākāhā to approximately 3 m, revealing the historic coral benthos. In support of their
333   hypothesis, kia'i loko noted an increase in fish aggregation around Kaho'okele over the course of
334   Pani ka Puka that has persisted.

335      Historically, the volume and location of surface water input into He'eia Fishpond from the Hoi
336   wetland and He'eia Stream was confined to flux through mākāhā. After the 1965 Keapuka flood,
337   however, damage to the kuapā and subsequent *R. mangle* growth resulted in an attenuated and
338   diffuse flow of fresh water into the loko i'a. Over this period of this study, Paepae o He'eia
339   commenced kuapā restoration along He'eia Stream and concomitant mangrove removal (Figure 1E)
340   in order to alter the path of surface water into the loko i'a. Kia'i loko posited that restoring the wall
341   and mākāhā would increase the rate of water exchange and flow rate, which might improve fish
342   passage into the estuary. *R. mangle* was initially removed from the remnant kuapā and nearby
343   fishpond interior by clear-cutting and incineration on site. With the exception of 2014-2015, the mean
344   rate of restoration was 154.84 ± 17.33 m yr-1, totaling 619.35 m kuapā (Table S5).

345   3.1.1 Characterizing mākāhā flux post-restoration (2018)

346      Four mākāhā along the eastern kuapā (Hīhīmanu, Kaho'okele, Nui, Kahoalāhui, Figure 2) were
347   assumed to have bi-directional flow mediated by the semi-diurnal tidal cycle in Kāne'ohe Bay. Three
348   mākāhā in the north and northwest sectors of He'eia Fishpond were documented since the early
349   1900s to provide conduits for surface water inputs into the loko i'a (Figure 1B). Wai 1 and Wai 2 were
350   restored over the course of this study. Wai 1 is located closest to the mouth of He'eia Stream and
351   allows the bidirectional exchange of fresh and oceanic water [30] whereas Wai 2, located 100 m
352   upstream, has a unidirectional flow of surface water into the loko i'a. The most upstream mākāhā
353   was destroyed during flood events in 1927 and 1965 and has not yet been restored and, measurements
354   with current meters in this area was not possible.

355      Meteorological conditions during water volume flux sampling events both pre- and post-
356   restoration have a small amount of variability (Table S2). While daily rainfall ranged from 0.05 cm to
357   1.32 cm in 2012 (pre-restoration) (mean 0.76 ± 0.6 cm), it ranged slightly higher from 0 cm-2.29 cm
358   (mean 1.23 ± 0.87) in 2018 (post-restoration). Similarly, Ha'ikū Stream discharge ranged from 0.04 $m^3$
359   $s^{-1}$- 0.07 $m^3$ $s^{-1}$ (mean 0.06 ± 0.013) in 2012 (pre-restoration), and from 0.06 $m^3$ $s^{-1}$-0.11 $m^3$ $s^{-1}$ (mean 0.085±
360   0.03) in 2018 (post-restoration). Wind direction ranged from E to NE (average wind direction ~50°)
361   with magnitude ranging from 10 to 13 knots pre-restoration and from E to NE (average wind
362   direction ~60°) with magnitudes of 3-13 knots post-restoration.

363      Flood tide onset and end were defined as low slack water (LSW, flux = 0 $m^3$ $s^{-1}$) tide stage and
364   high slack water (HSW, flux = 0 $m^3$ $s^{-1}$), respectively. Conversely, ebb tide onset and end were defined
365   as HSW and LSW, respectively. LSW levels range from 0.2 m at Kahoalāhui to 0.65 m at Kaho'okele
366   and Wai 1, whereas HSW levels range from ~0.5m at Kahoalāhui to 1.1 m at Kaho'okele. It is likely
367   that the water level at Wai 1 is consistently high due to continuous baseline stream flow.

368      Peak flux occurs mid-way between slack tides, thus the water level to water volume flux
369   relationship, the rating curve, typically resembles a "C" curve or vertical sine function. Rating curves
370   were generated to understand the influence of 4 tidal stages (Spring Flood, SF; Spring Ebb, SE; Neap
371   Flood, NF; and Neap Ebb, NE) on water volume flux ($m^3$ $s^{-1}$) and water level (m) for each mākāhā
372   with positive values corresponding to water volume flux into and negative values corresponding to
373   water volume flux out of the fishpond (Figure 2). We noted that Wai 2 exhibits an atypical rating
374   curve due to a wooden board in the mākāhā that restricts discharge into the loko i'a only when the
375   water level is higher than the board (Figure 2, Wai 2).

376      Mean and peak water volume flux was highest during flood tides at all mākāhā. The fastest
377   mean water volume flux (4.18 $m^3$ $s^{-1}$ at SF and 2.26 $m^3$ $s^{-1}$ at NF) and peak water volume flux (9.70 $m^3$
378   $s^{-1}$at SF and 5.41 $m^3$ $s^{-1}$ at NF) were recorded at mākāhā Nui, Table 3. In addition, flood tidal cycle
379   duration was shorter than ebb at all mākāhā at both Spring and Neap, mean tidal duration was 5.23
380   ± 1.20 hr and 8.00 ± 0.84 hr for SF and NF, respectively, whereas mean tidal duration was 6.09 ± 0.73

381  hr and 15.67 ± 1.38 hr for SE and NE respectively. Taken together, the shorter lag time at high water
382  vs. low water, longer-duration dropping tides and stronger flood than ebb currents suggest that
383  Heʻeia Fishpond is a flood-dominant system.

384  **Table 3.** Water flux dynamics in Heʻeia Fishpond post-restoration (2018).

| | Mean flux (m³ s⁻¹) | Peak flux (m³ s⁻¹) | Tidal cycle duration (hr) | Cum. flux per tidal cycle (m³) | Flux rate (m³ hr⁻¹) | Volume exchanged per tidal cycle (m³) | Relative flux |
|---|---|---|---|---|---|---|---|
| **Spring Flood** | | | | 191660 | 31778 | 191660 | 100.00% |
| Wai 2 | 0.05 | 0.16 | 4.43 | 840 | 190 | 840 | 0.44% |
| Wai1 | 0.40 | 0.93 | 4.55 | 7140 | 1569 | 7140 | 3.37% |
| Kahoalāhui | 1.47 | 0.92 | 4.36 | 24420 | 5601 | 24420 | 12.74% |
| Nui | 4.18 | 9.70 | 6.29 | 97800 | 15548 | 97800 | 51.03% |
| Kahoʻokele | 2.02 | 4.69 | 7.29 | 54380 | 7460 | 54380 | 28.37% |
| Hīhīmanu | 0.39 | 0.95 | 5.02 | 7080 | 1410 | 7080 | 3.69% |
| **Spring Ebb** | | | | -174880 | -30851 | −174880 | 100.00% |
| Wai 2 | 0.07 | -0.09 | 5.50 | 1560 | 284 | 1560 | −0.89% |
| Wai1 | -0.32 | -0.63 | 6.32 | -7600 | -1203 | −7600 | 4.35% |
| Kahoalāhui | -0.87 | -0.62 | 6.31 | -20220 | -3204 | −20220 | 11.56% |
| Nui | -3.60 | -4.86 | 5.53 | -76320 | -13801 | −76320 | 43.64% |
| Kahoʻokele | -1.10 | -3.12 | 5.50 | -67520 | -12276 | −67520 | 38.61% |
| Hīhīmanu | -0.17 | -0.43 | 7.35 | -4780 | -650 | −4780 | 2.73% |
| **Neap Flood** | | | | 141384 | 16717 | 141384 | 100.00% |
| Wai 2 | 0.05 | 0.20 | 7.41 | 1300 | 175 | 1300 | 0.92% |
| Wai1 | 0.32 | 0.98 | 8.29 | 9720 | 1172 | 9720 | 6.87% |
| Kahoalāhui | 0.51 | 0.36 | 7.31 | 13620 | 1863 | 13620 | 9.63% |
| Nui | 2.26 | 5.41 | 9.46 | 78744 | 8324 | 78744 | 55.70% |
| Kahoʻokele | 1.35 | 2.52 | 7.30 | 36440 | 4992 | 36440 | 25.77% |
| Hīhīmanu | 0.05 | 0.24 | 8.20 | 1560 | 190 | 1560 | 1.10% |
| **Neap Ebb** | | | | -159938 | -10584 | −159938 | 100.00% |
| Wai 2 | 0.88 | -0.09 | 17.46 | 5640 | 323 | 5640 | −3.53% |
| Wai1 | -0.17 | -0.57 | 15.50 | -9880 | -637 | −9880 | 6.18% |
| Kahoalāhui | -0.30 | -0.30 | 15.50 | -17100 | -1103 | −17100 | 10.69% |
| Nui | -1.60 | -3.19 | 14.09 | -81298 | -5770 | −81298 | 50.83% |
| Kahoʻokele | -0.86 | -1.80 | 17.10 | -53280 | -3116 | −53280 | 33.31% |
| Hīhīmanu | -0.08 | -0.25 | 14.34 | -4020 | -280 | −4020 | 2.51% |

385  3.1.2 Changes in relative water volume flux post-restoration

386       We evaluated the relative contribution of each mākāhā to loko iʻa water exchange during
387  SF, SE, NF, and NE in order to gain insight into how restoration altered circulation in Heʻeia
388  Fishpond. Prior to restoration, Ocean Break, the 0.9 m elbow wall bridging the 56 m gap in the eastern
389  kuapā was lower than the adjoining sections of wall, restricting water exchange to high tidal stages,
390  when the water level exceeded the height of Ocean Break.   The highest mean water volume flux at
391  all tidal states was measured at Nui, which accounted for roughly half of the total water volume
392  exchanged during one tidal cycle post-restoration (Table 3, Figure 3). The newly added mākāhā
393  channel at Kahoʻokele accounted for the second largest volume of water flux post-restoration with
394  roughly a quarter of influx and a third of outflux (Table 3, Figure 3). Kahoalāhui is comprised of three
395  individual mākāhā post-restoration and together they account for the third largest water volume -
396  roughly 10% of contribution to total water volume flux. The lowest water volume flux among the
397  ocean-influenced mākāhā was measured at Hīhīmanu with considerably lower mean velocities and
398  relative water flux contributions of < 5%. In 2018, flux rates measured at Wai 1 were similar to pre-
399  restoration with a relative flux magnitude of 3-7% and low mean flow rates (Figure 3). Wai 2
400  displayed unidirectional flow into the fishpond only, regardless of tidal state with solely positive
401  flow velocities and accounting for the lowest water volume flux measured.
402       When comparing site-specific volume flux rates pre-restoration (2012) to post-restoration (2018),
403  it becomes evident that the relative magnitude of water volume flux specific to each mākāhā changed
404  due to restoration practices: The total amount of water volume exchanged in a complete tidal cycle
405  decreased from 241,413 m³ pre-restoration to 194,700 m³ post-restoration for flood tide and decreased
406  from -241,685 m³ pre-restoration to -173,080 m³ post-restoration (Table 4). Pre-restoration, Ocean
407  Break facilitated the largest amount of volume exchange contributing approximately ~80% to total
408  water exchange at both flood and ebb tidal cycles (81.94% for flood, 79.76% for ebb) with mean water
409  velocities of 11.53 m³ s⁻¹ and -13.55 m³ s⁻¹ [39]. Pre-restoration, Nui contributed the second largest

410  amount of volume exchange with 12.88% for flood and 11.12% for ebb tide and mean velocities of
411  1.75 m³ s⁻¹ and -0.5 m³ s⁻¹ [39]. While contributing only 10% to water exchange pre-restoration, post-
412  restoration Nui is presently the site with largest water volume exchange. Post-restoration, Nui
413  facilitated about half of the volume exchanged (50.24% at flood tide, 44.1% at ebb tide) with much
414  higher mean water volume flux of 4.18 m³ s⁻¹ and -3.6 m³ s⁻¹ (Table 4) than pre-restoration. In contrast
415  to pre-restoration, Kahoʻokele now accounts for the second largest volume exchanged (27.93% and
416  39.01% for flood and ebb tide respectively) with lower mean water volume flux of 2.02 m³ s⁻¹ and -1.1
417  m³ s⁻¹ compared to pre-restoration. The relative contribution in the magnitude of three channels
418  constituting triple mākāhā increased about six-fold for flood tide and five-fold for ebb tide from pre-
419  restoration to post-restoration (from 1.71% to 12.54% for flood tide and 2.41% to 11.68% for the ebb

## FIGURE 3
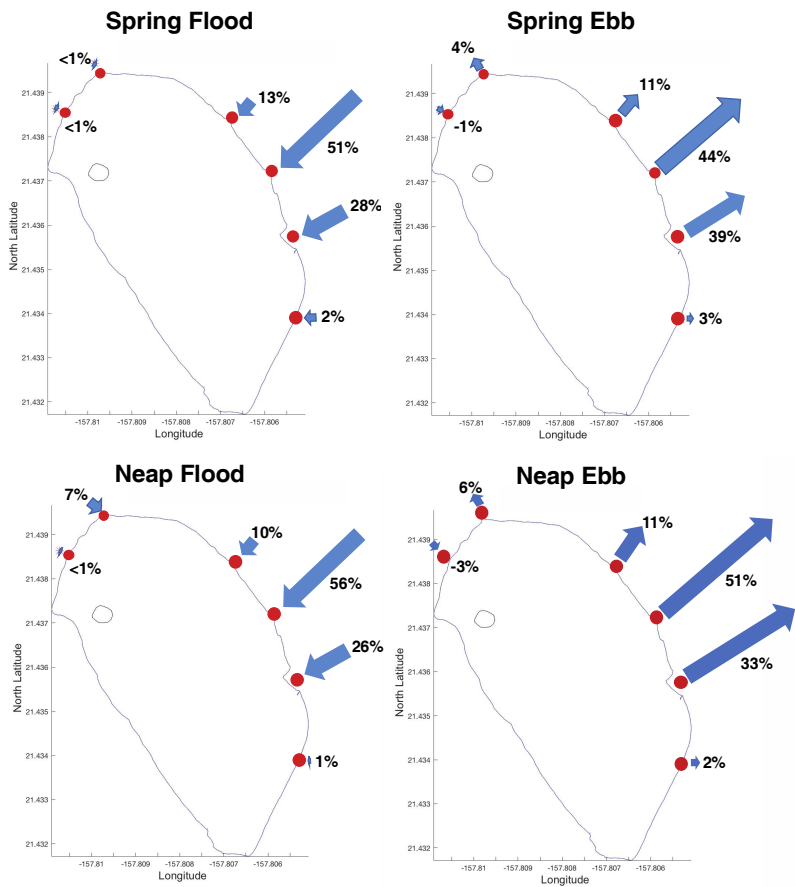


420  tide, Table 4). Hīhīmanu did not experience significant changes due to restoration: While accounting
421  for 1.69% at flood and 2.03% for ebb pre-restoration, it now accounts for 3.61% and 2.76% at flood
422  and ebb, respectively (Table 4). Mean water volume flux ranged from -0.12 m³ s⁻¹ to 0.28 m³ s⁻¹ pre-
423  restoration and are now -0.17 m³ s⁻¹ to 0.39 m³ s⁻¹.

424  **Figure 3. Relative water flux post-restoration dominated by Mākāhā Nui, and Mākāhā**
425  **Kahoʻokele.** Relative water flows through each mākāhā during spring flood tide; spring
426  ebb tide; neap flood tide; neap ebb tide. Arrow lengths are visual representations of the
427  relative magnitude of water flux at each mākāhā, normalized to the total flux for each
428  respective cycle. Mākāhā location, filled red circles.

429  In terms of overall volume exchange, the river mākāhā continue to play minor roles in water
430  exchange. Water volume flux at the two river mākāhā at Wai 1 overall has increased from pre-
431  restoration to post-restoration: Water passing through Wai 1 increased from 0.93% pre-restoration to
432  5.1% post-restoration for flood tide, and 2.4% pre-restoration to 5.7% post-restoration for ebb tide.
433  Water volume flux increased from 0.09 m³ s⁻¹ and 0.1 m³ s⁻¹ pre-restoration to 0.4 m³ s⁻¹ and 0.32 m³ s⁻¹
434  post-restoration. Pre-restoration Wai 2 accounted for 0.85% of water exchange during flood tide and

435 accounts for a slightly decreased water exchange of 0.67% post-restoration for flood tide. For ebb tide,
436 the water exchange reversed from 2.28% pre-restoration to -3.25% post-restoration.
437     Restoration resulted in a significant shift in water exchange in the seaward kuapā. Prior to
438 restoration, Ocean Break accounted for the most water exchange during spring tide (~80%) whereas
439 post-restoration, the relative contribution of Kahoʻokele was nearly one-third, at ~30% water
440 exchange. Instead, Nui now exchanges the greatest water exchange, ~50%. Thus, the spatial pattern
441 of flushing in Heʻeia Fishpond remains dominated by the mākāhā in the northeast quadrant of the
442 loko iʻa for all tidal stages. Nui, Kahoʻokele, and Kahoalāhui together contributing for a water
443 exchange of 92% of water volume at spring flood, 94% at spring ebb, 91% at neap flood and 95% at
444 neap ebb tide whereas the southern and eastern edges of the fishpond experience relatively low
445 flushing.

446     **Table 4.** Change in flux rates through mākāhā pre-restoration (2012) and post-restoration
447     (2018).

| | Flood Tide | | | | Ebb Tide | | | |
|---|---|---|---|---|---|---|---|---|
| | Pre-restoration | | Post-restoration | | Pre-restoration | | Post-restoration | |
| **Mākāhā** | Volume exchange per tidal cycle (m³) | Relative flux | Volume exchange per tidal cycle (m³) | Relative flux | Volume exchange per tidal cycle (m³) | Relative flux | Volume exchanged per tidal cycle (m³) | Relative flux |
| Wai 2 | 2057 | 0.85% | 1300 | 0.67% | −5515 | 2.28% | 5640 | −3.25% |
| Wai 1 | 2249 | 0.93% | 9720 | 5.10% | −5791 | 2.40% | −9880 | 5.70% |
| Kahoalāhui | 4106 | 1.71% | 24420 | 12.54% | −5802 | 2.41% | −20220 | 11.68% |
| Nui | 31101 | 12.88% | 97800 | 50.24% | −26886 | 11.12% | −76320 | 44.10% |
| Kahoʻokele/OB | 197820 | 81.94% | 54380 | 27.93% | −192780 | 79.76% | −67520 | 39.01% |
| Hīhīmanu | 4081 | 1.69% | 7080 | 3.61% | −4912 | 2.03% | −4780 | 2.76% |
| Mākāhā Total | 241,413 | 100.00% | 194,700 | 100.00% | −241,685 | 100.00% | −173,080 | 100.00% |

448 *3.2 Decrease in loko iʻa volume and residence time post-restoration*

449     The majority of the loko iʻa has relatively uniform and shallow bathymetry of ~0.9 m with the
450 deeper portions around the mangrove island and Ocean Break [26]. Prior to restoration, water
451 exchange along the eastern kuapā only occurred when the water depth exceeded the height of the
452 elbow wall at Ocean Break. Pre-restoration, ~90% of loko iʻa water exchange occurred in the northeast
453 corner of the fishpond via Ocean Break (~80%) and Nui (~10%), suggesting that the eastern half of the
454 fishpond was better mixed and less stratified than the western side of the fishpond [30], Timmerman
455 *et al*, unpublished. Water volume exchange before restoration was also found to be largely tidally
456 driven, with the greatest volume exchange at midtide: ~77% during spring tide and ~42% during
457 neap tide.
458     Given changes in flux in Heʻeia Fishpond due to restoration, we determined post-restoration
459 loko iʻa volume and residence time for SF, SE, NF, NE. Heʻeia Fishpond is deepest during SF tide
460 (Figure 4A), averaging 0.89 ± 0.12 m with a minimum water depth of 0.63 m in the center of the loko
461 iʻa and a maximum water depth of 1.46 m around the mangrove island in the northwestern corner
462 of the fishpond. During SF, the maximal volume of the loko iʻa is 264,730 m³ (Figure 4B).   The
463 minimum water volume occurs during SE tide when the loko iʻa is 48,060 m³ or 20% of the SF volume
464 (Figure 4B). The mean fishpond depth at spring ebb tide is 0.17 m ± 0.12 m and ranges from 0 m in
465 the fishpond center to 0.74 m around the mangrove island in the northwestern corner of the fishpond.
466 The NF tidal volume is 149,550 m³, 56% of the SF tidal volume, with a mean depth of 0.50 m ± 0.12,
467 ranging from 0.25 - 1.08 m. NE depth ranges from 0 - 0.79 m, averaging 0.22 ± 0.12 m. NE tidal volume
468 is 63,160 m³. Restoration regimes resulted in a considerable change of loko iʻa volume from pre-
469 (2007) to post-restoration (2018): SE tide fishpond volume decreased 16,010 m³, SF volume decreased
470 17,990 m³, NE volume decreased 14,890 m³ and NF volume increased 15,660 m³ (Figure 4B). Thus, as
471 a result of removing the elbow wall and installing a sixth mākāhā (Kahoʻokele), Heʻeia Fishpond is
472 shallower and has a lower volume at all tidal states except NF.
473     We calculated that post-restoration, approximately 82% of the fishpond water is exchanged
474 during the ebb-flood transition at spring tide. During the neap tide ebb-flood transition, 58% of the
475 fishpond water is exchanged. To be consistent with previous work by Young [30], we defined one

476 flushing cycle as the time that it takes to flush out 82% of fishpond water during spring ebb tide and
477 to replenish that water again with new Kāneʻohe Bay water during spring flood tide or 12 hr. Based
478 on the assumption that the incoming water would mix uniformly with the water remaining in the
479 loko iʻa during the first flushing cycle (18%), about 3 flushing cycles are required to mix the initial
480 18% of water to a <1% dilution. Therefore, the post-restoration minimum residence time of Heʻeia
481 Fishpond is ~ 32 hr or under 3 flushing cycles, and occurs during spring tide when water exchange is
482 maximal. In contrast, when water exchange is minimal (e.g., neap tides), the maximum residence
483 time is 64 hr. More than 5 flushing cycles or 64 hr are required to mix the 42% of water retained down
484 to <1% dilution. Water exchange during ebb flood transition experienced a 4.51% increase (from
485 77.34% pre-restoration to 81.85% post-restoration, Table 4) at spring tide. During neap tide water
486 exchange increased 16.06% (from 41.71% pre-restoration to 57.77% post-restoration, Table 4). As a

**FIGURE 4**
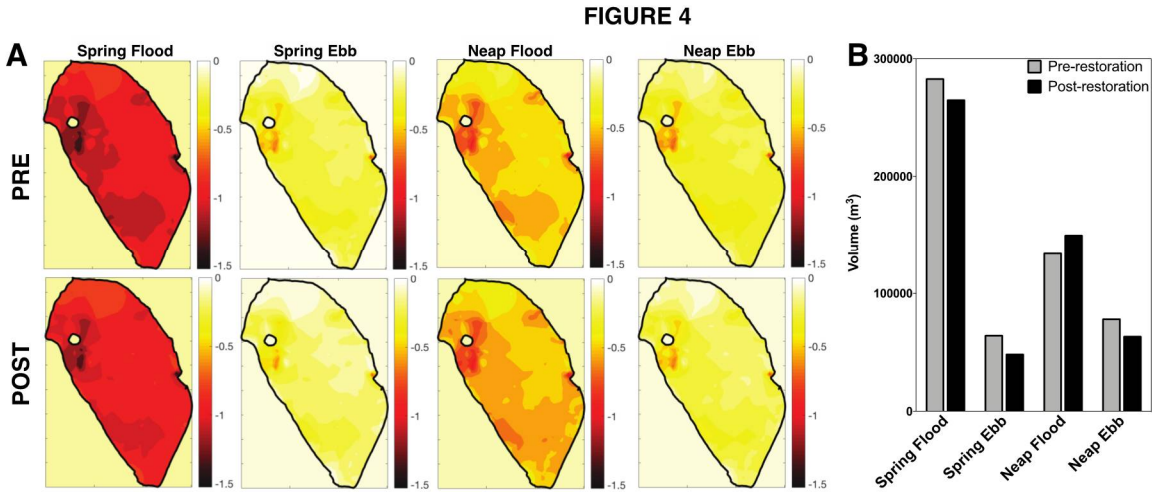


487 result, minimum water residence time decreased from 38 hours at spring tide pre-restoration to 32
488 hours (~1.5 days) at spring tide post-restoration and maximal residence time during neap tides
489 decreased from 102 hours (~8.5 days) at spring tide pre-restoration to 64 hours (~5.5 days) at spring
490 tide post-restoration.

491 **Figure 4. Comparison of Heʻeia Fishpond depth and volume pre- vs. post-restoration**
492 **over various tidal stages.** (**A**) Fishpond depth (m) for spring flood, spring ebb, neap flood,
493 neap ebb pre-restoration (top row) vs. post-restoration (bottom row). (**B**) Fishpond volume
494 (m³) for each tidal stage pre-restoration (grey) vs. post-restoration (black).

495 *3.3 Spatial salinity distribution significantly altered due to restoration*

496 The water column geochemistry of Heʻeia Fishpond is influenced by the mixing of distinct
497 water masses: surface water from Heʻeia Stream, whose discharge depends on precipitation;
498 submarine groundwater discharge, comprised of a mixture of fresh water from an underground
499 aquifer and recirculated seawater [31]; and seawater from Kāneʻohe Bay that fluctuates with tidal
500 pumping. Built at the interface of Heʻeia Stream and Kāneʻohe Bay, Heʻeia Fishpond exhibits a
501 typical vertical salinity gradient - a less dense, freshwater lens atop a more dense, saltier water mass
502 - although mixing of these water masses does occur with increased river flow, winds, and tides. A
503 major motivation for the biocultural restoration of Heʻeia Fishpond was to increase the freshwater
504 influence in the loko iʻa. Kiaʻi loko hypothesized that brackish conditions would drive primary
505 production of diatoms - a major food source for juvenile mullet, which is a target species. Surface and
506 bottom salinities were measured using a handheld YSI at several locations in Heʻeia Fishpond
507 (Figure 5A). We selected two pre-restoration sampling events from 2014 and three post-restoration
508 sampling events from 2017 with similar meteorological conditions (Table S3 and S4). Salinity
509 measurements from pre and post-restoration work were analyzed as an indicator of fishpond
510 circulation, mixing, and stratification.
511 Surface salinity distribution pre- and post-restoration display a strong spatial gradient (Figure
512 5B, left panels). The highest salinities in both cases were measured along the ocean-ward kuapā near
513 Nui and the Ocean Break/Kahoʻokele (station P10), while the lowest salinity was measured along

514   He'eia Stream near Wai 2 (station P3, L07). However, mean pre-restoration salinity was significantly
515   higher than post-restoration salinity, 27.4 ± 4.86 ppt and 20.5 ± 10.41 ppt, respectively (p-value < 0.01).
516   With similar meteorological conditions, these data indicate a weaker freshwater influence and
517   stronger salinity gradient pre-restoration. Before restoration, the freshwater wedge did not extend
518   past the western edge of the mangrove island, where salinities ranged from 20 – 25 ppt (stations P2,
519   P4, P5) and further west, salinities rose to 25 – 30 ppt (stations P1, P6, P7, P8, P9). Post-restoration
520   however, salinity ranged from 0.10 – 32.59 ppt with the freshwater wedge from the river extended
521   beyond the mangrove island, which ranged from 15 – 20 ppt (stations L06, L08, L09), with further
522   west salinities rising to above 20 ppt (station L01 and L05) and 25 – 30 ppt (stations L02, L03, L04,
523   L11, M03). The presence of strong spatial gradient throughout the restoration process suggests that
524   freshwater from He'eia Stream is more prevalent along the northwestern side of the loko i'a,
525   whereas tidal pumping from Kāne'ohe Bay dominates the southeastern side of the loko i'a.

526       As expected, bottom waters of the loko i'a had a higher salinity than the surface, however, post-
527   restoration salinity exhibited limited gradient structure post-restoration, whereas the loko i'a bottom
528   pre-restoration was entirely homogeneously mixed with no detectable freshwater influence (Figure
529   5B, right panels). Mean bottom salinities were significantly higher pre-restoration (31.99 ± 1.82 ppt)
530   as compared to post-restoration (25.17 ± 8.12 ppt), p-value < 0.1. Post-restoration, the influence of
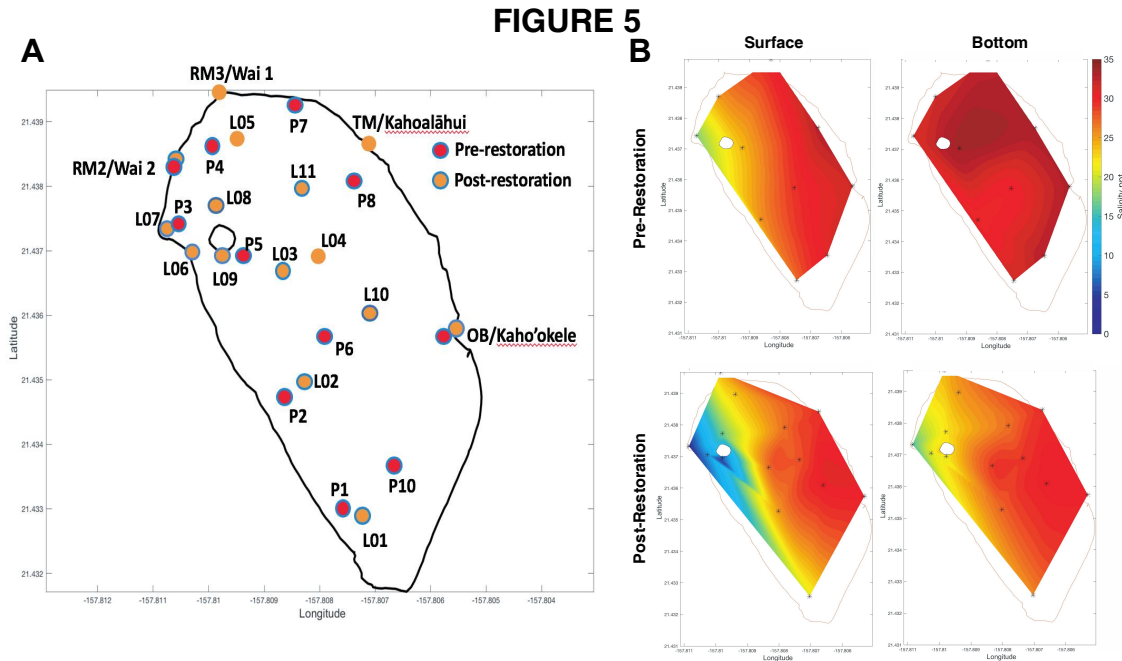
**FIGURE 5**



531   freshwater from He'eia Stream became more evident, with the majority of the loko i'a salinity
532   ranging from 20-25 ppt (Figure 5B, lower right panel). Similar to the surface salinity spatial
533   distribution, highest measurements were taken near the Kaho'okele and Nui and the lowest
534   measured bottom salinities were taken at Wai 2.

535       **Figure 5. Average salinity of He'eia Fishpond surface and bottom waters decreased due**
536       **to restoration. (A)** Discrete sampling sites for microbial indicator species in the water
537       column (blue circles) and/or salinity (pre-restoration, red fill, and post-restoration, orange
538       fill). **(B)** Heat map of salinity as a proxy for the relative proportion of freshwater and ocean
539       water in the fishpond. Gradient of higher salinity in the eastern sectors of the fishpond
540       bordering Kāne'ohe Bay and lowest salinity near the diffusive flow region closest to He'eia
541       Stream and the unrestored portion of kuapā is typical of an estuarine saltwater wedge.

542   *3.4 Restoration-driven changes to circulation altered microbial biomarker spatial distribution*

543       To understand the consequences of Paepae o He'eia's restoration regime on biological-physical
544   interactions in the loko i'a, we quantified the abundance of microbial biomarkers that have been used
545   previously to track fecal contamination within bodies of water. We focused on 3 specific bacterial

546  groups: *Enterococcus* and Bacteroidales, indicators of contamination from mammals and *C.*
547  *marimammalium*, an indicator for contamination from avian sources, to investigate how increasing
548  freshwater inputs into the loko iʻa potentially affect the biogeography of pathogens.
549      Discrete samples were collected from a network of stations across the loko iʻa along a transect
550  from Wai 2 to Kahoʻokele to capture the salinity gradient observed previously (Figure 5A, L03, L06,
551  L07, L09, L10). In addition, we sampled at a higher resolution around the mangrove island on the
552  interior of the fishpond in order to consider the influence of the large *B. ibis* rookery housed in the *R.*
553  *mangle* stand. Contrary to expectations, amplification of the 16S rDNA genes from the family
554  Bacteroidales (GenBac3) and the genus *Enterococcus* (Entero 1a) from samples pre- and post-
555  restoration showed no significant difference when averaged across all stations (Figure 6A). We
556  hypothesized that grouping together data may have masked changes in biomarker spatial
557  distribution that occurred due to restoration. We mapped the mean concentration (16S copies 100 mL$^{-}$
558  $^{1}$) onto the stations and used a rectangular grid with ~1 m spacing to determine whether the
559  biogeography of *Enterococcus* and Bacteroidales changed from 2014 to 2017 (Figure 6B and 6C
560  respectively). We found that prior to restoration, the mean concentration of *Bacteroidales* was higher
561  than 10$^4$ copies per 100 mL across the entire western side of the loko iʻa. In contrast, post-restoration,
562  Bacteroidales concentrations higher than 10$^4$ copies per 100 mL were restricted to a geographically
563  smaller area of the fishpond, adjacent to Wai 2 and the diffuse flow region and lower in the center of
564  the loko iʻa (Fig 6B and 6C, top row). Indeed, when grouped by salinity, freshwater stations showed
565  a statistically significant decrease in Bacteroidales concentration post-restoration (Figure 6D, top row,
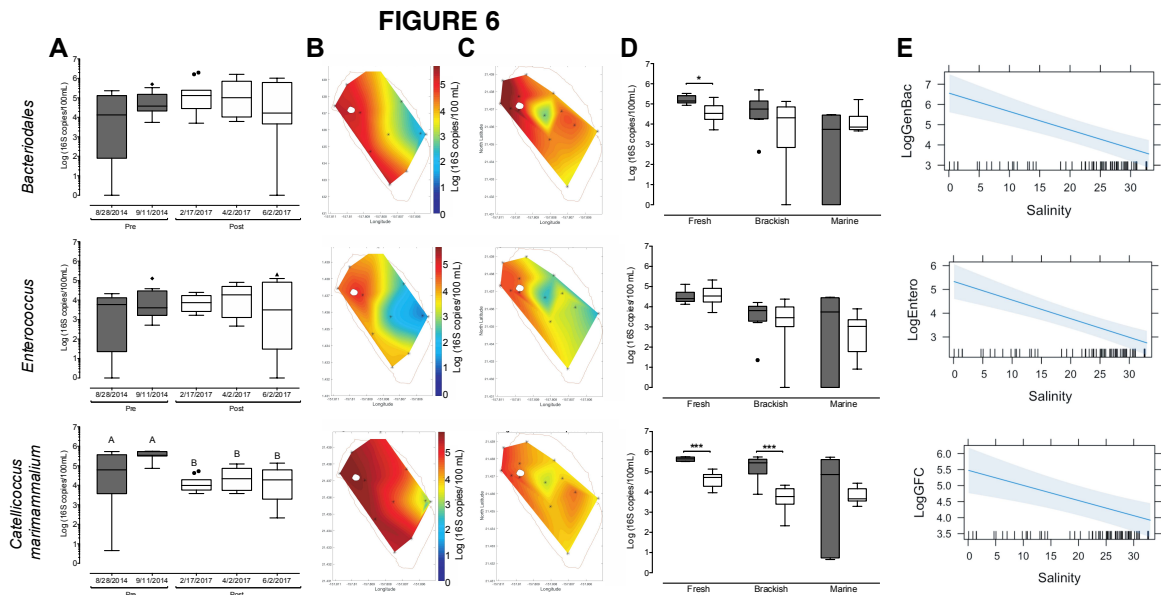


**FIGURE 6**

566  white). GAMM analysis confirmed that concentration of Bacteroidales negatively correlates with
567  salinity (Figure 6E, top row), with the highest concentrations found at stations with the lowest
568  salinity.

569  **Figure 6. Spatial distribution and mean concentration of *Bacteroidales*, *Enterococcus* and**
570  ***Fusobacteria* pre- and vs. post-restoration. (A)** Tukey box-plot diagrams showing
571  concentration, log (16S copies/100 mL)of *Bacteroidales* (GenBac3), *Enterococcus* (Entero1a),
572  and *Fusobacteria* (GFC) for before (grey) and after (white) fishpond wall restoration from all
573  sampling sites, outliers and 95% confidence intervals are indicated. Heat maps of the
574  averaged abundance of pre-restoration (**B**) and post-restoration (**C**) date *Bacteroidales*
575  (GenBac3), *Enterococcus* (Entero1a), and *Fusobacteria* (GFC). Tukey box plot diagrams of
576  Bacteroidales (GenBac3), *Enterococcus* (Entero1a), and *Fusobacteria* (GFC) abundance binned
577  by salinity (freshwater, brackish and marine) of sites pre- and post-restoration, 95%
578  confidence intervals and outliers are indicated. **(D)** Tukey box-plot diagrams showing

579    concentration, log (16S copies/100 mL) of *Bacteroidales* (GenBac3), *Enterococcus* (Entero1a),
580    and *Fusobacteria* (GFC) for before (grey) and after (white) fishpond wall restoration binned
581    by salinity.   Outliers and 95% confidence intervals are indicated, * $p < 0.05$, *** $p \ll 0.001$.
582    (**E**) Correlation between salinity and biomarker concentration using a generalized additive
583    mixed model.

584    We also found that when values were grouped across all stations *Enterococcus* concentrations
585    did not change significantly over the course of restoration (Figure 6A, middle row). However, unlike
586    Bacteroidales, the spatial distribution of *Enterococcus* pre- and post-restoration were structured with
587    highest concentrations along the western edge of the loko iʻa ($10^4$ copies per 100 mL) and a decreasing
588    gradient proceeding to the east down to $10^2$ - $10^3$ copies per 100 mL (Figure 6B and 6C, middle row).
589    The lack of difference in pre- vs post-restoration data was also supported by binning the stations
590    along a salinity gradient (Figure 6D, middle row). As expected, the general additive mixed model
591    (Figure 6E, middle row) confirmed that *Enterococcus* has increased survival in low salinity
592    environments.
593    To assess *B. ibis* fecal contamination, we first developed microbial source tracking tools by
594    adapting primers specific to the 16S rDNA gene of *C. marimammalium* (Table 2, GFCf and GFCr).
595    These primer pairs had previously been used to detect fecal contamination from gulls, geese, ducks,
596    and chickens [38]. GFC primers specifically amplified fecal DNA from *B. ibis* living at Heʻeia
597    Fishpond (Figure S1) and were used to determine the extent of contamination from *B. ibis* fecal
598    sources in the loko iʻa. Pre-restoration, *B. ibis* fecal contamination was significantly higher across all
599    stations (mean concentrations of 2-4 x $10^5$ copies 100 ml$^{-1}$) as compared to $10^4$ copies 100 ml$^{-1}$ post-
600    restoration (Fig 6A, bottom row), $p < 0.01$. In general, the spatial distribution of pre- and post-
601    restoration *B. ibis* fecal indicator bacteria had weak correlations with co-registered salinity
602    measurements (Figure 5). Pre-restoration concentrations of *B. ibis* fecal indicator bacteria were higher
603    across all stations than both *Bacteroidales* and *Enterococcus* (Figure 6B), with greater than $10^3$ copies
604    per 100 mL detected at the oceanic stations. In contrast, post-restoration concentrations of *C.
605    marimammalium* decreased by 2 orders of magnitude, and these differences were statistically
606    significant at the fresh and brackish stations (Figure 6D, bottom row). GAMM indicate that while the
607    negative correlation between *B. ibis* fecal indicator bacteria and salinity is not as strong as with
608    Bacteroidales and *Enterococcus*, it does exist.
609    We note 2 interesting differences in microbial indicator concentrations and biogeography post-
610    restoration. First, we note the appearance of a region where microbial indicator concentrations are
611    low (Figure 6C). We note that differences in the station locations pre- vs post-restoration may have
612    altered the interpolation of biomarker concentrations. Alternatively, this may suggest that post-
613    restoration, circulation patterns in the center of the fishpond have resulted in a well-flushed zone.
614    Secondly, all three molecular markers exhibited high variability 16S copy concentration pre-
615    restoration as compared to post-restoration at the marine stations (Figure 6D). We interpret this
616    difference as an indication that pre-restoration, the loko iʻa was less homogeneously mixed than
617    post-restoration.

## 4. Discussion

619    Embedded between land and sea, Heʻeia Fishpond is a powerful natural laboratory. We have
620    been provided the unique opportunity to examine how historical land use change has altered the
621    functions of coastal habitats and how biocultural restoration maintains and improves the integrity of
622    these coastal ocean ecosystems in the face of rapid global change. In the current study, we utilized a
623    comprehensive time series dataset of *in situ* deployments, discrete sampling, and empirical
624    observations to draw a link between restoration efforts and changing fishpond circulation, as well as
625    water quality dynamics. Specifically, we examined the impact of invasive mangrove removal around
626    the northern fishpond periphery from 2014-2017 and Pani ka Puka, repair of the Ocean Break in 2015,
627    presenting a comparison of pre- vs. post-restoration ecosystem dynamics along multiple parameters.

628    *4.1 Hoʻoniho ka niho[1]: Water volume flux changes due to kuapā repair*

629        Generally, understanding the physical environment of Heʻeia Fishpond will advance our
630    knowledge of the dynamic biochemical and physical interactions in Hawaiian estuarine ecosystems.
631    In repairing the physical infrastructure of Heʻeia Fishpond, Paepae o Heʻeia have set the stage for
632    the ecology of the loko iʻa to return to the original conditions engineered by *kūpuna* (elders, ancestors)
633    of Heʻeia: a brackish body of water with a consistent volume, maintained by regulated mixing of
634    fresh and marine inputs to facilitate phytoplankton growth. Our study confirms that during baseline
635    conditions, coastal loko iʻa circulation patterns are primarily driven by a combination of either tidal
636    pumping or stream velocity, depending on the location of the mākāhā [30,41]. Flux rates during SF
637    and SE tides from mākāhā bordering Kāneʻohe Bay (Hīhīmanu, Kahoʻokele, Nui, Kahoalāhui),
638    suggest that the fishpond is more influenced by oceanic inputs (> 95% total mean flux) than
639    freshwater inputs (< 5% total mean flux) from Heʻeia Stream during baseline conditions at both pre-
640    and post-restoration (Tables 3 and 4, Figure 3).
641        Prior to Pani ka Puka, Heʻeia Fishpond acted largely as an unconfined system during spring
642    tides, when the spring flood tide exceeded the height of Ocean Break. In essence, because the Ocean
643    Break was lower in height than the surrounded kuapā, the entire 56 m wide section of Ocean Break
644    functioned like a mākāhā when tidal pumping in Kāneʻohe Bay was higher than the provision elbow
645    wall. Pre-restoration, we observed enormous water volume flux at spring tides, ~80% exchange
646    almost exclusively from Ocean Break (Table 4). However, during neap tides, the loko iʻa was more
647    confined with less exchange and circulation in the southeastern portion of the fishpond. In 2015, this
648    expansive section of the wall was repaired and Kahoʻokele was built, shifting relative mākāhā
649    exchange rates at Kahoʻokele to ~30% post-restoration. This dynamic is also reflected in mean water
650    volume flux rates: Pre-restoration, Ocean Break had the highest mean water volume flux rates of ~12-
651    14 $m^3s^{-1}$ (Table 4), while the Kahoʻokele flux rates post-restoration are dramatically lower (now ~ 1
652    $m^3s^{-1}$, Tables 3 and 4). Mean water volume flux rates at other mākāhā generally increased from pre-
653    restoration to post-restoration, an indication that nearby mākāhā somewhat compensate for the
654    difference in flux between Ocean Break and Kahoʻokele. However, the general "C" shape of rating
655    curves remained similar (Figure 3). In its current state, the addition of Kahoʻokele renders Heʻeia
656    Fishpond a confined system at all tidal states with adequate water exchange in the southeastern
657    region. These findings are supported by Ertekin *et al.* [42] who modeled circulation patterns at two
658    different Aliʻi fishponds in Molokaʻi, which concluded that the number of mākāhā plays a
659    significant role in improving tidal circulation. They concluded that mākāhā distance and location in
660    relation to the physical forces at work (tidal activity, wind, fishpond bathymetry, stream location)
661    affected circulation inside the fishpond.
662        Our results suggest that oceanic mākāhā water volume flux is also dependent upon wind
663    forcing, in particular for mākāhā aligned with the trade winds (~70°). Nui and Kahoʻokele account
664    for ~50% and ~30% of total flux respectively, Figure 3. These mākāhā also have the largest cross-
665    sectional areas (Nui: 6.48 m; Kahoʻokele: 3.05 m, Table 1), and are positioned most in-line with the
666    predominant trade wind direction, Nui has a bearing of 63° and Kahoʻokele has a bearing of 80°
667    (Table 1). Wind blowing from the northeast across Kāneʻohe Bay, can accelerate (if the wind aids) or
668    dampen (if the wind opposes) water flow through Nui and somewhat Kahoʻokele, which is aligned
669    with the predominant wind direction of 70°. We also noted that the channel floor of Kahoʻokele is
670    deeper than the adjacent benthos of both the loko iʻa interior and Kāneʻohe Bay. Thus, the mākāhā
671    floor depth may allow slightly higher flux through Kahoʻokele due to lower resistance to water
672    volume flux. In contrast, Kahoalāhui and Hīhīmanu have considerably smaller relative flux (together
673    accounting for ~ 15%, Figure 3) as the individual channels of Kahoalāhui have small cross-sectional
674    areas and Hīhīmanu has the smallest cross-sectional area (2 m, Table 1), in addition to being
675    positioned at 48° and 111°, respectively. The notion that wind can influence the rate of water flow
676    through mākāhā is supported by a study by Yang [43] who suggested that the rate of water flow
677    through the mākāhā may be altered by wind accelerating or dampening flow when the body of water
678    was large enough. Kāneʻohe Bay and Heʻeia Fishpond are both large enough, and shallow enough
679    to be affected by wind stress in such a way as to act as a secondary driver of flux in this system.

---

[1] Interlock the stones [40]

680 　　　　We found that the river mākāhā have significantly lower relative flux rates during base flow
681 conditions pre- and post-restoration (Wai 1 and Wai 2 together ~5%). Flux through Wai 1, the most
682 seaward mākāhā along the Heʻeia Stream, is affected by tidal activity due to its proximity to
683 Kāneʻohe Bay, making it the only freshwater mākāhā that allows bi-directional water flow. Under
684 baseline conditions, the relative flux of water passing through Wai 1 during flood tide is balanced by
685 the amount of water flowing back out during ebb tide (Table 3). At flood tides, flowing out of Wai 1
686 is dampened by Heʻeia Stream, flowing in the opposite direction into the loko iʻa, while Heʻeia
687 Stream flow is additive during ebb tides. Due to a dam-like structure in the mākāhā (Figure 2), Wai
688 2 has little to no detectable tidal signal and exhibit exclusive unidirectional flow from Heʻeia Stream
689 into the loko iʻa that is largely dependent stream discharge and precipitation in the Heʻeia watershed
690 [30,41,43]. During episodic storm events, strong freshwater influx can have pronounced effects on
691 the fishpond system [30], yet our flux measurements were all conducted at baseline/low flow
692 conditions. We anticipate that the relative contribution of river mākāhā vs. ocean mākāhā, as well as
693 the balance between ebb vs. flood exchange, is likely to change if Heʻeia Stream discharge increases
694 during storm events. Research comparing baseline to storm conditions to quantify how higher stream
695 velocities affect loko iʻa flushing is currently underway and will be the subject of a subsequent
696 contribution.
697 　　　　Assuming the Heʻeia Fishpond water balance is in steady state, the influx rates should be
698 equivalent to outflux rates. However, we found the difference between spring and neap tidal cycle
699 flow, the sum of flow (m³) for all mākāhā, to be -16,760 m³ or ~8% of total flow between SF and SE
700 tide and 18,554 m³ or ~13% of total flow between NF and NE (Table 4). Post-restoration, this imbalance
701 is most evident in 2 mākāhā: Kahoʻokele, which accounts for 28% of influx, and 39% of outflux during
702 spring tide, and Nui, which accounts for 40% of influx and 44% of outflux during spring tide. This
703 pattern is evident at both spring and neap tidal cycles. We posit that trade winds accelerate flow into
704 the fishpond at Nui during flood tide, which as previously discussed is aligned with the prevailing
705 wind direction during sampling (63°, Table 1). However, during ebb tide, the wind force opposes
706 outflow at Nui, and a small proportion of water flux is redistributed to other mākāhā channels
707 thereby compensating for the reduced outflow at Nui (Table 3, Figure 4). However, these site-specific
708 differences do not account for all the discrepancy observed pre- and post-restoration. We attribute
709 discrepancies in flux balances to a number of factors. First, the influence of submarine groundwater
710 discharge (SGD) into Heʻeia Fishpond is not accounted for in this study. Previous work quantifying
711 SGD at Heʻeia Fishpond using radon isotope measurements found that the amount of water flux
712 from SGD was equal to that of Heʻeia Stream discharge [31,44]. Second, the flux in the diffuse flow
713 region (Figure 1B), as well as gains or losses of water through small holes in the kuapā, was not able
714 to be quantified and has not been accounted for in our water budget. In addition, though every effort
715 was made to choose tidal cycles similar in length and amplitude for rating curves, rating curves were
716 calculated using *in situ* data from sequential rather than simultaneous deployments due to the
717 limitation of instruments (Table S1). Some degree of variability in tidal length and amplitude among
718 sites likely exists. Finally, the mixed semidiurnal tides cause large variations in tidal length (Table 3),
719 giving rise to some uncertainty in the final water volume flux rates calculated.

720 *4.2 Paepae ke alo[2]: Volume, residence time, and salinity*

721 　　　　Pani ka Puka affected loko iʻa volumes and residence times considerably (Figure 4). The
722 addition of a sixth mākāhā (Kahoʻokele) led to increased and faster outflux during both NE and SE
723 tides, corresponding to lower volumes post-restoration. Conversely, whereas no water exchange
724 occurred at Ocean Break during neap tides prior to restoration, Kahoʻokele allows more influx
725 during NF tide compared to before, resulting in a larger loko iʻa volume post-restoration during this
726 tidal stage (Figure 4). These increased water masses cannot be compensated entirely with the flow (1
727 - 2 m³s⁻¹) through Kahoʻokele, which has a smaller cross-diameter, 3.05 m as compared to Ocean
728 Break, 56 m (Figure 1C and 1D). We predicted a decrease in residence time post-restoration,
729 particularly during neap tides Kahoʻokele enables water exchange at all tidal states. We found that
730 total exchange rates increased 5% during spring tides between pre- and post-restoration, and

---

2 Raise the face of the wall [40]

731  minimum residence time during this tidal stage decreased 12% from 38 hr to 32 hr. For neap tides,
732  water exchange increased 16% and maximum residence time decreased 37% from 102 hr pre-
733  restoration to 64 hr post-restoration. These data are tempered the following assumptions made in
734  order to calculate residence time:   (1) uniform mixing of the loko iʻa water column, (2) all flood and
735  ebb tides are 6 hours long, (3) mākāhā present the only source of water exchange. However, from
736  salinity measurements at surface vs. bottom, it is evident that the water column is sometimes mildly
737  stratified and not homogeneously mixed. Furthermore, upon analyzing the variability in length of
738  tidal cycles, it becomes clear that there is a large range in variability (from 4.43 - 17.46 hr for tidal
739  cycle duration, Table 3). Lastly, it is likely that there are other indirect sources of water exchange as
740  SGD and the diffuse flow region. The difference in minimum and maximum residence times
741  emphasizes the importance of differentiating between tidal states when looking at the effects of
742  restoration on the physical environment of the loko iʻa.

743      Concomitant mangrove removal around the stream mouth corresponded with an increase in
744  water volume flowing through Wai 1 from ~1-2% pre-restoration to ~5% post-restoration (Figure 1E
745  and Table 4) and a freshening of the loko iʻa post-restoration. At the end of the period of this study,
746  Wai 2 was not fully clear of *R. mangle* and also showed little change in discharge between pre- and
747  post-restoration. We conclude that mangrove removal positively correlates with increased water flow
748  and subsequently improved loko iʻa circulation. Increased freshwater flux is also reflected in the
749  salinity distribution, which shows a much stronger freshwater signal around the river mākāhā in
750  post-restoration compared to pre-restoration (Figure 5B). We expect that continued removal of
751  mangrove along the loko iʻa periphery will increase stream velocity and the mass of freshwater
752  entering Heʻeia Fishpond. Moreover, the temperature of the surface water is often much lower than
753  marine inputs and given concerns about fish stress linked to sea surface warming trends [29], mixing
754  of cooler water may be beneficial to fish survival. In addition, increased freshwater and nutrient input
755  may be beneficial for native macroalgae and phytoplankton to thrive, which is the primary food
756  source for the herbivorous target fish species. While we can only speculate as to the historical
757  biogeochemistry of Heʻeia Fishpond, the abundance of evidence suggests that increasing freshwater
758  input is necessary for proper management of native marine species. As this is the first study we are
759  aware of that reveals a correlation between mangrove removal and improved loko iʻa circulation, we
760  recommend long-term monitoring of fish and phytoplankton diversity and biomass, particularly near
761  the stream so that the connection between mangrove removal, stream flow, and nearshore fishery
762  health can be fully understood.

763  *4.3 Pani hakahaka[3]: Microbial indicators as markers of watershed connectivity*

764      To assess water quality and associated human health risk, we used two broad-spectrum
765  microbial bioindicators used by the US Environmental Protection Agency [45,46]. We used primers
766  that targeted the Bacteroidales family (GenBac3) and the *Enterococcus* genus (Entero1a), bacteria that
767  are common in the feces of mammals, Table 2. These non-pathogenic microbes are easy to quantify
768  and have decay rates similar to those of the pathogens of interest [47], hence, they can be strongly
769  associated with the presence of pathogenic microorganisms derived from upstream in the watershed.
770  By performing co-registered sampling of salinity and microbes, we were able to directly correlate
771  fecal indicator concentrations with salinity, an abiotic factor that strongly influences survival rates
772  [45,48,49]. We hypothesized that shorter residence time and increased water volume flux would
773  lower the concentration of Bacteroidales and *Enterococcus* in Heʻeia Fishpond. Instead, we found no
774  significant overall difference in surface mammalian fecal indicator bacteria before and after
775  restoration (Figure 6A). We found coherence between spatial distribution of mammalian fecal
776  indicators with surface salinity (Figure 6B): post-restoration, lower salinity (e.g. more fresh water) in
777  the northwestern sector of the loko iʻa corresponded with even higher concentrations of surface
778  bioindicators as compared to pre-restoration whereas higher salinity in the oceanic-dominated areas
779  of the fishpond had even less fecal contamination than pre-restoration. As mammalian fecal
780  contaminants are introduced via terrigenous freshwater runoff, the increase in river flushing detected
781  post-restoration, we attribute the increase in mammalian fecal bacteria in the northwest area of the

---

[3]  Close gaps/vacancies [40]

782 loko iʻa to increased stream input. It is possible that mammalian indicator bacteria may accumulate
783 in the freshwater lens at the surface of the fishpond, bacterial concentrations in bottom waters need
784 to be considered. Because the expansion of freshwater niches are generally more favorable for these
785 microbes to survive [49], these results emphasize the need for enhanced pollution reduction
786 management upstream.
787      We also evaluated an internal source of fecal pollution deriving from a large colony of *B. ibis*
788 residing on the mangrove island on the loko iʻa interior. In order to quantify *B. ibis* fecal
789 contamination, we optimized primers to *C. marimammalium* (GFC, Table 2), an uncharacterized Gram-
790 positive facultative anaerobe in the order of *Lactobacillales (Fusobacterium)* [50] originally developed
791 to detect fecal contamination from gulls in coastal environments [38,51–53] for cattle egret fecal
792 material (Figure S1). Unlike Bacteroidales and *Enterococcus*, we found a significant decrease in egret
793 fecal bacteria post-restoration, suggesting that increased flushing and decreased residence times had
794 a positive impact on water quality. The pattern of decreasing *C. marimammalium* and consistent
795 abundance of Bacteroidales and *Enterococcus* between the pre- and post-repair periods is intriguing
796 and may be related to differential environmental reservoirs of the two clades targeted by the assays.
797 GenBac3 and Entero1a are phylogenetically very broad probes that target a diverse clade of
798 organisms that may contain unknown members with variable salinity tolerances. In contrast, the GFC
799 probes target a specific organism with few environmental isolates having a narrower range of salinity
800 tolerance. As the cattle egret colony on the mangrove island is the primary source of bird fecal
801 contamination to the fishpond, eliminating egret habitat by removing the mangrove island is
802 expected to further reduce the amount of contamination from bird feces.
803      As Hawaiian watersheds are highly interconnected, loko iʻa provide snapshots of ecosystem
804 health for the entire ahupuaʻa. Fecal contamination in our study site confirms the presence of leaking
805 cesspools and/or septic tanks in the Haʻikū and ʻIolekaʻa watersheds. This kind of pollution
806 endangers plans for seafood production as well the public, who participate in numerous educational
807 and cultural activities.

808 *4.4 Pōhaku ka papale[4]: Future Implications of revitalizing customary fishpond infrastructure*

809      Since initiating wall restoration in 2005, Paepae o Heʻeia recognized the necessity of fixing
810 Ocean Break in order to have a functioning fishpond. While aquaculture was possible using net pens,
811 conventional methods were labor-intensive, expensive, and did not allow the entire 88 acres of the
812 loko iʻa to be utilized for rearing fish. Large-scale fish mortality events in 2009, wherein only fish in
813 the net pens died, served to further support the organization's desire to return to traditional
814 cultivation methods.   The process to obtain the necessary federal and state permits to begin
815 reconstruction took over three years. Importantly, the kiaʻi loko of Heʻeia Fishpond made the
816 decision that restoring the Ocean Break would be an undertaking for the entire community, not just
817 the organization. This approach to restoration not only revitalized the physical structure of the loko
818 iʻa but revitalized the traditional Hawaiian practice of coming together as a community to maintain
819 these cultural sites. Serendipitously, completion of the kuapā and Kahoʻokele coincided with the 50th
820 anniversary of the Keapuka flood, further affirming the appropriateness of taking a biocultural
821 approach toward stewardship of this loko iʻa.
822      The design of the new kuapā with additional mākāhā represents an innovation of the
823 contemporary kiaʻi loko to mitigate future flooding risk. While deviating from historical
824 photographs from the 1920s, it is likely that over the course of the 800-year existence of Heʻeia
825 Fishpond kuapā infrastructure has been altered in response to hydrological and oceanic conditions.
826 Kelly noted archeological evidence that the kuapā adjacent to Heʻeia Stream has been moved
827 multiple times, potentially due to catastrophic floods [22], suggesting that placement and number of
828 mākāhā were dynamically managed. Paepae o Heʻeia revealed more contemporary evidence of this
829 during the restoration of Nui, when concrete slotted mākāhā, likely built in the 1900s, was found
830 buried in the kuapā interior. Because kiaʻi loko were concerned about future floods and the integrity
831 of a 3 m wall, they reasoned that having a mākāhā would facilitate the release of water pressure
832 during high flow events. The exact location of the mākāhā was based on practitioner knowledge of

---

[4] Place the capstone on the top [40]

833  the circulation and biological diversity of the area. Thus, re-establishment of customary practices
834  encompassed adaptation for increased resilience, as well as future fish recruitment.

835  A key dimension to restoring He'eia Fishpond has been the removal of invasive *R. mangle*,
836  whose roots grow into the kuapā, separating the rock and coral. Furthermore, mangrove roots hold
837  sediment transported from upstream and its leaf litter directly contribute to the organic matter in the
838  pond, changing the chemistry of the benthos and water column. Mangrove canopies acted as a wind
839  block, impeding circulation and oxygenation, creating heterogenous micro-niches within the loko
840  i'a. Moreover, kia'i loko observed that this non-native species also corresponded with the presence
841  of non-native fish, and they speculated that mangrove removal would enable native aquaculture
842  species to compete more effectively in this habitat, potentially by increasing fish passage into the
843  estuary. Examining the rates of sediment transport from the loko i'a out to Kāne'ohe Bay is needed,
844  as well as a more comprehensive understanding of how this introduced species functions in non-
845  native vs native landscapes.

846  Overall, this study clearly demonstrates the positive impact restoration regimes had on various
847  physical and microbiological components of the fishpond ecosystem. Our results are encouraging
848  and indicate that there is a significant potential for community-based restoration to revitalize this,
849  and other, culturally and economically significant sites for sustainable aquaculture in the future.
850  More recently, in part because of the ongoing concerted efforts of community organizations like
851  Paepae o He'eia, the coastal area of He'eia was designated as National Estuarine Research Reserve
852  (NERR) in January 2017 to advance research and protection of the He'eia ahupua'a by integrating
853  the traditional Hawaiian ecosystem management approach with contemporary estuarine
854  management practices.

879  ## References

880  1.    Mathieson, A. M. The state of world fisheries and aquaculture. *World review of fisheries and aquaculture* **2012**.
881  2.    Loke, M. K.; Geslani, C.; Takenaka, B.; Leung, P. Seafood consumption and supply sources in Hawaii, 2000-
882        2009. *Mar. Fish. Rev.* **2012**, *74*, 44–51.
883  3.    Keala, G.; Hollyer, J. R. *LOKO I'A*; College of Tropical Agriculture and Human Resources, University of
884        Hawai'i Mānoa, 2007; pp. 1–76;.

885     4.    Kikuchi, W. K. Prehistoric hawaiian fishponds. *Science* **1976**, *193*, 295–299, doi:10.1126/science.193.4250.295.

886     5.    Cobb, J. N. *The Commercial Fisheries of the Hawaiian Islands in 1903*; U.S. Government Printing Office, 1905;.

887     6.    Keala, G.; Hollyer, J. R.; Castro, L. Loko Ia: A manual on Hawaiian fishpond restoration and management.
888           *University of Hawaii at Mānoa, Honolulu, Hawaii* **2007**.

889     7.    Munro, G. C. Island of Moloka 'i. *First Report of the Board of Commissioners of Agriculture and Forestry of the*
890           *Territory of Hawaii for the Period from July* **1904**, *1*, 94–96.

891     8.    Gedan, K. B.; Kirwan, M. L.; Wolanski, E.; Barbier, E. B.; Silliman, B. R. The present and future role of coastal
892           wetland vegetation in protecting shorelines: answering recent challenges to the paradigm. *Clim. Change*
893           **2011**, *106*, 7–29, doi:10.1007/s10584-010-0003-7.

894     9.    Twilley, R. W.; Lugo, A. E.; Patterson-Zucca, C. Litter production and turnover in basin mangrove forests
895           in southwest Florida. *Ecology* **1986**, *67*, 670–683.

896     10.   Chimner, R. A.; Fry, B.; Kaneshiro, M. Y.; Cormier, N. Current Extent and Historical Expansion of
897           Introduced Mangroves on O'ahu, Hawai'i. *Pac. Sci.* **2006**, *60*, 377–383, doi:10.1353/psc.2006.0013.

898     11.   Allen, J. A. Mangroves as Alien Species: The Case of Hawaii. *Global Ecol. Biogeogr. Lett.* **1998**, *7*, 61–71,
899           doi:10.2307/2997698.

900     12.   Drigot, D. C. Mangrove removal and related studies at Marine Corps Base Hawaii. *Tech Note M-3N in*
901           *technical notes: Case studies from the Department of Defense conservation program. US Dept. of Defense Legacy*
902           *Resource Management Program Publication* **1999**, 170–174.

903     13.   Walsh, G. E. An ecological study of a Hawaiian mangrove swamp. *Estuaries* **1967**, *83*, 420–431.

904     14.   Crooks, J. A. Characterizing ecosystem-level consequences of biological invasions: the role of ecosystem
905           engineers. *Oikos* **2002**, *97*, 153–166.

906     15.   Demopoulos, A. W. J.; Fry, B.; Smith, C. R. Food web structure in exotic and native mangroves: a Hawaii–
907           Puerto Rico comparison. *Oecologia* **2007**, *153*, 675–686, doi:10.1007/s00442-007-0751-x.

908     16.   Sweetman, A. K.; Middelburg, J. J.; Berle, A. M.; Bernardino, A. F.; Schander, C.; Demopoulos, A. W. J.;
909           Smith, C. R. Impacts of exotic mangrove forests and mangrove deforestation on carbon remineralization
910           and ecosystem functioning in marine sediments. *Biogeosciences* **2010**, *7*, 2129–2145, doi:10.5194/bg-7-2129-
911           2010.

912     17.   Wester, L. Introduction and Spread of Mangroves in the Hawaiian Islands. *Yearbook of the Association of*
913           *Pacific Coast Geographers* **1981**, *43*, 125–137, doi:10.1353/pcg.1981.0006.

914     18.   Force, H. G. M. S. T.; Matsuoka, J. K. *Hawaii. Governor's Molokaʻ i Subsistence Task Force Final Report*; Task
915           Force, 1994;.

916     19.   Matsuoka, J. K.; McGregor, D. P.; Minerbi, L. Molokai: A study of Hawaiian subsistence and community
917           sustainability. *Sustainable community development: Studies in economic, environmental, and cultural*
918           *revitalizations. CRC Press, Boca Raton, Florida* **1998**, 25–44.

919     20.   Farber, J. M. *Ancient Hawaiian Fishponds: Can Restoration Succeed on Moloka'i?*; Neptune House Publications
920           Encinitas, Calif, USA, 1997;.

921     21.   Declaration of Hui Malama Loko Iʻ a. In; 2012.

922     22.   Kelly, M. *Loko I'a O He'eia: Heeia Fishpond*; Department of Anthropology, Bernice P. Bishop Museum, 1975;.

923     23.   Banner, A. H. *A fresh-water" kill" on the coral reefs of Hawaii*; Hawaii Institute of Marine Biology, University
924           of Hawaii, 1968;.

925     24.   Water      Levels      -      NOAA      Tides      &      Currents      Available      online:
926           https://tidesandcurrents.noaa.gov/waterlevels.html?id=1612480&units=standard&bdate=19650101&edate
927           =19651201&timezone=GMT&datum=MLLW&interval=m&action=data (accessed on Sep 15, 2018).

928     25.   Brooks, M. He'eia Fishpond. In *Proceedings of The Governor's Moloka'i Fishpond Restoration Workshop*; Wyban,
929           C. A., Ed.; Office of Hawaiian Affairs, 1991; pp. 20–24.

930     26.   Vasconcellos, S. M. K. *Distribution and Characteristics of a Photosynthetic Benthic Microbial Community in a*
931           *Marine Coastal Pond*; University of Hawaiʻ i Mānoa, 2007;.

932     27.   Scott, T. M.; Rose, J. B.; Jenkins, T. M.; Farrah, S. R.; Lukasik, J. Microbial source tracking: current
933           methodology and future directions. *Appl. Environ. Microbiol.* **2002**, *68*, 5796–5803.

934     28.   Kirs, M.; Kisand, V.; Wong, M.; Caffaro-Filho, R. A.; Moravcik, P.; Harwood, V. J.; Yoneyama, B.; Fujioka,
935           R. S. Multiple lines of evidence to identify sewage as the cause of water quality impairment in an urbanized
936           tropical watershed. *Water Res.* **2017**, *116*, 23–33, doi:10.1016/j.watres.2017.03.024.

937     29.   McCoy, D.; McManus, M. A.; Kotubetey, K.; Kawelo, A. H.; Young, C.; D'Andrea, B.; Ruttenberg, K. C.;
938           Alegado, R. A. Large-scale climatic effects on traditional Hawaiian fishpond aquaculture. *PLoS One* **2017**,

939    *12*, e0187951, doi:10.1371/journal.pone.0187951.

940   30.   Young, C. W. Perturbation of Nutrient Level Inventories and Phytoplankton Community Composition
941      During Storm Events in a Tropical Coastal System: Heʻeia Fishpond, Oʻahu, Hawaiʻi. Masters of Science,
942      University of Hawaiʻi Mānoa, 2011.

943   31.   Kleven, A. Coastal Groundwater Discharge as a Source of Nutrients to Heʻeia Fishpond, Oʻahu, HI.
944      Bachelor of Science, University of Hawaiʻi at Mānoa, 2014.

945   32.   Ludwig, W.; Schleifer, K. H. How quantitative is quantitative PCR with respect to cell counts? *Syst. Appl.*
946      *Microbiol.* **2000**, *23*, 556–562, doi:10.1016/S0723-2020(00)80030-2.

947   33.   Haugland, R. A.; Siefring, S. C.; Wymer, L. J.; Brenner, K. P.; Dufour, A. P. Comparison of Enterococcus
948      measurements in freshwater at two recreational beaches by quantitative polymerase chain reaction and
949      membrane filter culture analysis. *Water Res.* **2005**, *39*, 559–568, doi:10.1016/j.watres.2004.11.011.

950   34.   *Method 1611: Enterococci in Water by TaqMan® Quantitative Polymerase Chain Reaction (qPCR) Assay*; United
951      States Environmental Protection Agency Office of Water (4303T), 2012;.

952   35.   Dick, L. K.; Field, K. G. Rapid estimation of numbers of fecal Bacteroidetes by use of a quantitative PCR
953      assay for 16S rRNA genes. *Appl. Environ. Microbiol.* **2004**, *70*, 5695–5697, doi:10.1128/AEM.70.9.5695-
954      5697.2004.

955   36.   Siefring, S.; Varma, M.; Atikovic, E.; Wymer, L.; Haugland, R. A. Improved real-time PCR assays for the
956      detection of fecal indicator bacteria in surface waters with different instrument and reagent systems. *J.*
957      *Water Health* **2008**, *6*, 225–237, doi:10.2166/wh.2008.022.

958   37.   *Method B: Bacteroidales in Water by TaqMan® Quantitative Polymerase Chain Reaction (qPCR) Assay*; United
959      States Environmental Protection Agency Office of Water (4303T), 2010;.

960   38.   Green, H. C.; Dick, L. K.; Gilpin, B.; Samadpour, M.; Field, K. G. Genetic markers for rapid PCR-based
961      identification of gull, Canada goose, duck, and chicken fecal contamination in water. *Appl. Environ.*
962      *Microbiol.* **2012**, *78*, 503–510, doi:10.1128/AEM.05734-11.

963   39.   Moehlenkamp, P. Kū Hou Kuapā: Increase of water exchange rates and changes in microbial source
964      tracking markers resulting from restoration regimes at Heʻeia Fishpond. M.S., University of Hawaiʻi
965      Mānoa, 2018.

966   40.   Heʻeia, P. o. *Hoʻoniho ka niho*; 2015;.

967   41.   Ertekin, R. C.; Yang, L.; Sundararaghavan, H. *Hawaiian Fishpond Studies: Web Page Development and the Effect*
968      *of Runoff from the Streams on Tidal Circulation*; 1999; pp. 1–53;.

969   42.   Ertekin, R. C. Molokai fishpond tidal circulation study. *Final report submitted to the University of Hawaii Sea*
970      *Grant College Program* **1996**.

971   43.   Yang, L. *A Circulation Study of Hawaiian Fishponds*; University of Hawaii, Department of Ocean and
972      Resources Engineering, 2000;.

973   44.   Dulai, H.; Kleven, A.; Ruttenberg, K.; Briggs, R.; Thomas, F. Evaluation of Submarine Groundwater
974      Discharge as a Coastal Nutrient Source and Its Role in Coastal Groundwater Quality and Quantity. In
975      *Emerging Issues in Groundwater Resources*; Advances in Water Security; Springer, Cham, 2016; pp. 187–221
976      ISBN 9783319320069.

977   45.   Noble, R. T.; Lee, I. M.; Schiff, K. C. Inactivation of indicator micro-organisms from various sources of faecal
978      contamination in seawater and freshwater. *J. Appl. Microbiol.* **2004**, *96*, 464–472.

979   46.   Shanks, O. C.; Kelty, C. A.; Sivaganesan, M.; Varma, M.; Haugland, R. A. Quantitative PCR for genetic
980      markers of human fecal pollution. *Appl. Environ. Microbiol.* **2009**, *75*, 5507–5513, doi:10.1128/AEM.00305-09.

981   47.   Murphy, H. Persistence of pathogens in sewage and other water types. *Global Water Pathogens Project. Part*
982      **2017**, *4*.

983   48.   Ortega, C.; Solo-Gabriele, H. M.; Abdelzaher, A.; Wright, M.; Deng, Y.; Stark, L. M. Correlations between
984      microbial indicators, pathogens, and environmental factors in a subtropical Estuary. *Mar. Pollut. Bull.* **2009**,
985      *58*, 1374–1381, doi:10.1016/j.marpolbul.2009.04.015.

986   49.   Shehane, S. D.; Harwood, V. J.; Whitlock, J. E.; Rose, J. B. The influence of rainfall on the incidence of
987      microbial faecal indicators and the dominant sources of faecal pollution in a Florida river. *J. Appl. Microbiol.*
988      **2005**, *98*, 1127–1136, doi:10.1111/j.1365-2672.2005.02554.x.

989   50.   Sinigalliano, C. D.; Ervin, J. S.; Van De Werfhorst, L. C.; Badgley, B. D.; Ballesté, E.; Bartkowiak, J.; Boehm,
990      A. B.; Byappanahalli, M.; Goodwin, K. D.; Gourmelon, M.; Griffith, J.; Holden, P. A.; Jay, J.; Layton, B.; Lee,
991      C.; Lee, J.; Meijer, W. G.; Noble, R.; Raith, M.; Ryu, H.; Sadowsky, M. J.; Schriewer, A.; Wang, D.; Wanless,
992      D.; Whitman, R.; Wuertz, S.; Santo Domingo, J. W. Multi-laboratory evaluations of the performance of

Catellicoccus marimammalium PCR assays developed to target gull fecal sources. *Water Res.* **2013**, *47*, 6883–6896, doi:10.1016/j.watres.2013.02.059.

51. Ryu, H.; Griffith, J. F.; Khan, I. U. H.; Hill, S.; Edge, T. A.; Toledo-Hernandez, C.; Gonzalez-Nieves, J.; Santo Domingo, J. Comparison of gull feces-specific assays targeting the 16S rRNA genes of Catellicoccus marimammalium and Streptococcus spp. *Appl. Environ. Microbiol.* **2012**, *78*, 1909–1916, doi:10.1128/AEM.07192-11.

52. Cloutier, D. D.; McLellan, S. L. Distribution and Differential Survival of Traditional and Alternative Indicators of Fecal Pollution at Freshwater Beaches. *Appl. Environ. Microbiol.* **2017**, *83*, doi:10.1128/AEM.02881-16.

53. Lee, C.; Marion, J. W.; Lee, J. Development and application of a quantitative PCR assay targeting Catellicoccus marimammalium for assessing gull-associated fecal contamination at Lake Erie beaches. *Sci. Total Environ.* **2013**, *454-455*, 1–8, doi:10.1016/j.scitotenv.2013.03.003.